ExtreMe Matter Institute (EMMI)

4th Workshop on Anti-Matter, Hyper-Matter and Exotica Production at the LHC

Bologna (Italy) February 13 -17, 2023

Extreme Matter in Neutron Stars and in related astrophysical phenomena

Ignazio Bombaci

Dipartimento di Fisica “E. Fermi”, Università di Pisa

and

INFN, Sezione di Pisa

The **EOS of extreme dense and hot matter** is a basic ingredient to describe a variety of astrophysical phenomena

- **Core-Collapse Supernovae**
- **Neutron star birth (protoneutron stars)**
- **Neutron Stars structure**
- **Meriging of Binary Neutron Stars (BNS) and**
- **Gravitational Wave (GW) signals from these mergers**

Using a complementary strategy

Observational data from the above mentioned astrophysical phenomena give us a unique opportunity to test our present models of the EOS of extreme matter.

Summary of the talk

- **EOS of nuclear matter and Neutron Stars (Nucleon Stars)**

  a. **Basic requirements of nuclear matter EOS models (empirical saturation properties, measured NS masses, … etc…..)**

  b. **Dependence of the nuclear matter EOS on the quantum many-body approach.**

- **Hyperons in dense matter and** (a possible solution of) **the hyperon puzzle**

- **Quark Matter in Neutron Stars and in BNS mergers.**

Neutron Stars: bulk properties

Mass	$M \sim 1.5\, M_\odot$
Radius	$R \sim 10$ km
Centr. Density	$\rho_c = (4 - 8)\, \rho_0$
Compactness	$R/R_g \sim 2 - 4$
Baryon number	$A \sim 10^{57}$
Binding energy	$B \sim 10^{53}$ erg

$B/A \sim 100$ MeV $\quad$ **$B/(Mc^2) \sim 10\%$**

Stellar structure: General Relativity

Giant "atomic nucleus" or "hypernucleus" bound by gravity

$M_\odot = 1.989 \times 10^{33}$ g $\quad R_\odot = 6.96 \times 10^5$ km $\quad R_{g\,\odot} = 2.95$ km

$\rho_0 = 2.6 \times 10^{14}$ g/cm^3 ($n_0 \sim 0.16$ fm^{-3} nuclear saturation density)

$R_g \equiv 2GM/c^2$ (Schwarzschild radius)

Atomic Nuclei: bulk properties

Mass number	$A = 1 - 238$ (natural stable isotopes)
Radius	$R = r_0 A^{1/3} \sim (2 - 8)$ fm
Density	$\rho \sim \rho_0 = 2.6 \times 10^{14}$ g/cm^3

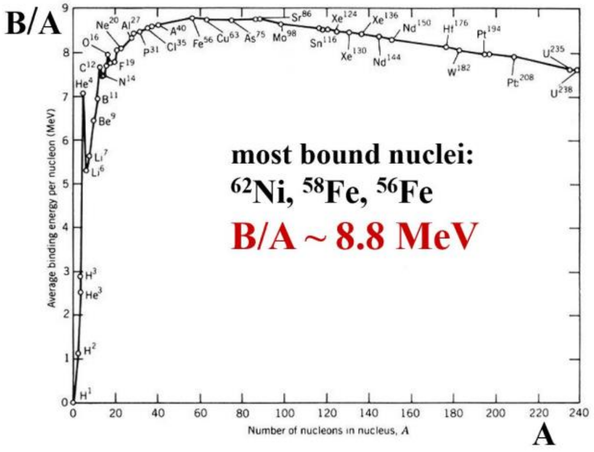

most bound nuclei: ^{62}Ni, ^{58}Fe, ^{56}Fe

$B/A \sim 8.8$ MeV

$B/(Mc^2) \sim (0.1\text{–}1)\%$

bound by nuclear interactions

Relativistic equations for stellar structure

Static and sphericaly symmetric self-gravitating mass distribution

Tolman – Oppenheimer – Volkov equations (TOV)

$$\frac{dP}{dr} = -G \frac{m(r)\rho(r)}{r^2}\left(1 + \frac{P(r)}{c^2\rho(r)}\right)\left(1 + 4\pi \frac{r^3 P(r)}{m(r)\; c^2}\right)\left[1 - \frac{2Gm(r)}{c^2\; r}\right]^{-1}$$

$$\frac{dm}{dr} = 4\pi r^2 \rho(r)$$

$$\frac{d\Phi}{dr} = -\frac{1}{\rho(r)c^2}\frac{dP}{dr}\left(1 + \frac{P(r)}{\rho(r)c^2}\right)^{-1}$$

One needs the **equation of state (EOS) of dense matter, P = P(ρ),** up to **very high densities**

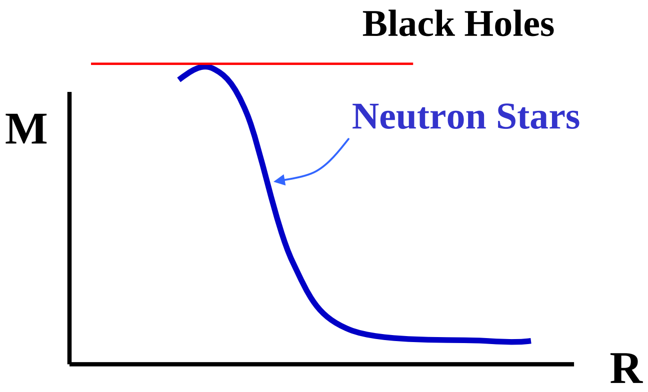

M_{max}**(EOS) ≥ all measured neutron star masses**

Measured Neutron Star masses in relativistic binary systems: three "heavy" Neutron Stars

Measuring post-Keplerian parameters: very accurate NS mass measurements;
model independent measurements within GR

PSR J1614–2230 $M_{NS} = 1.97 \pm 0.04\ M_\odot$

NS – WD binary system (He WD) $M_{WD} = 0.5\ M_\odot$ (companion mass)

$P_b = 8.69$ hr (orbital period) $P = 3.15$ ms (PSR spin period) $i = 89.17° \pm 0.02°$ (inclination angle)

P. Demorest et al., Nature 467 (2010) 1081

PSR J0348+0432 $M_{NS} = 2.01 \pm 0.04\ M_\odot$

NS – WD binary system $M_{WD} = 0.172 \pm 0.003\ M_\odot$ (companion mass)

$P_b = 2.46$ hr (orbital period) $P = 39.12$ ms (PSR spin period) $i = 40.2° \pm 0.6°$ (inclination angle)

Antoniadis et al., Science 340 (2013) 448

PSR J0740+6620 ($M_{NS} = 2.14^{+0.10}_{-0.09}\ M_\odot$) $M_{NS} = 2.08 \pm 0.007\ M_\odot$

NS – WD binary system $M_{WD} = 0.258\ M_\odot$ (companion mass)

$P_b = 4.7669$ days (orbital period) $P = 2.89$ ms (PSR spin period) $i = 87.38° \pm 0.20°$ (inclination angle)

(H. T. Cromartie et al., Nature Astronomy 4 (2020) 72) E. Fonseca et al, ApJL 915 (2021) L12

Measured Neutron Star Masses

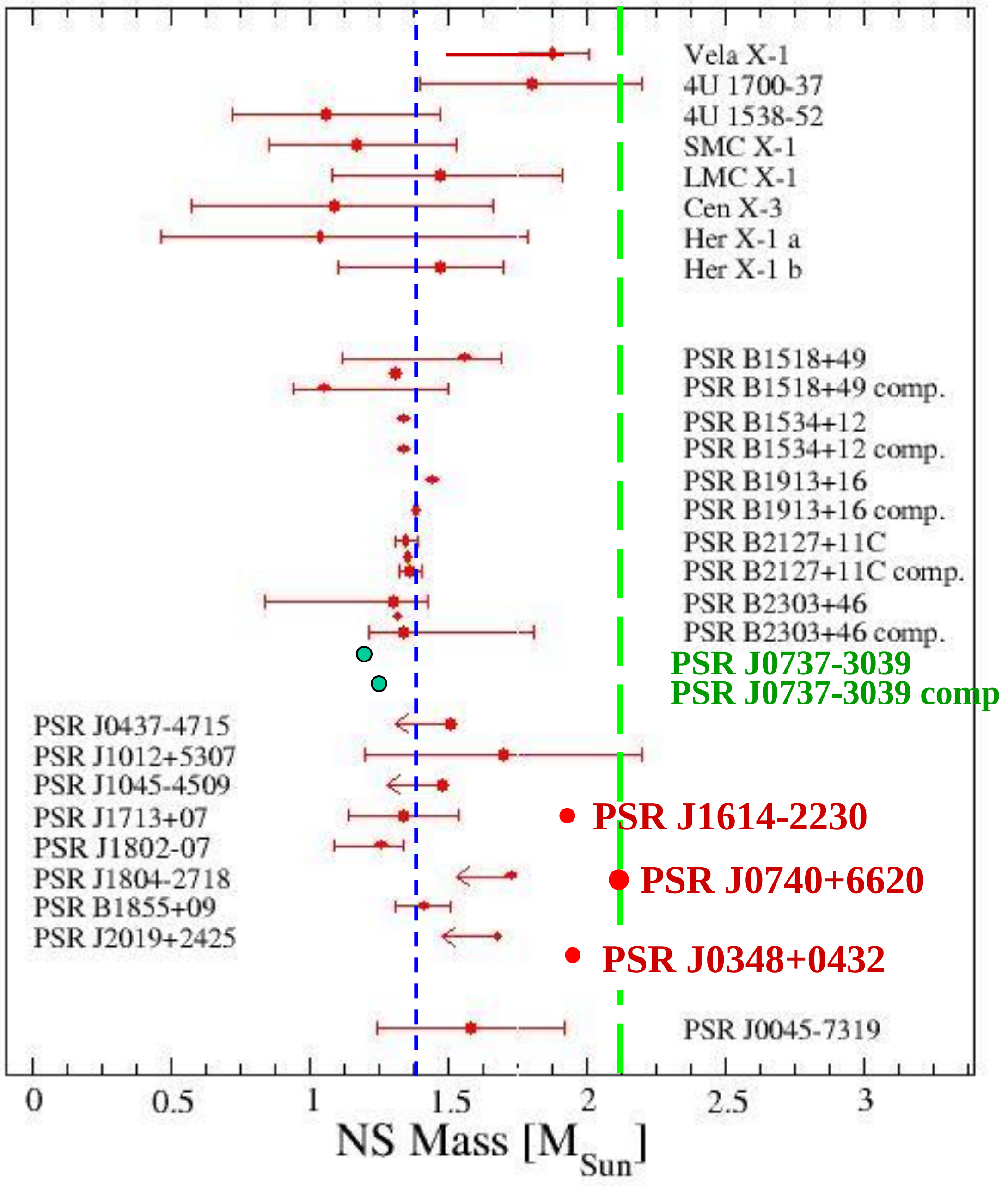

$M_{max} \geq 2\,M_{\odot}$

Very stringent constraint on the EOS

soft EOS are ruled out

Neutron star physics in a nutshell

1) **Gravity** compresses matter at very high density

2) **Pauli principle**

Stellar constituents are different species of **identical fermions** (n, p,...,e^-, μ^-)

⟶ antisymmetric wave function for particle Exchange ➔ Pauli principle

Chemical potentials $\mu_n, \mu_p, \ldots \mu_e$ rapidly increasing functions of the density

3) **Weak interactions** change the **isospin** and **strangeness** content of dense matter to **minimize the energy**

Cold catalyzed matter (Harrison, Wakano, Wheeler, 1958)

The ground state (minimum energy per baryon) of a system of hadrons and leptons with respect to their mutual strong and weak interactions at a given total baryon density n and temperature T = 0.

"Neutron Stars"

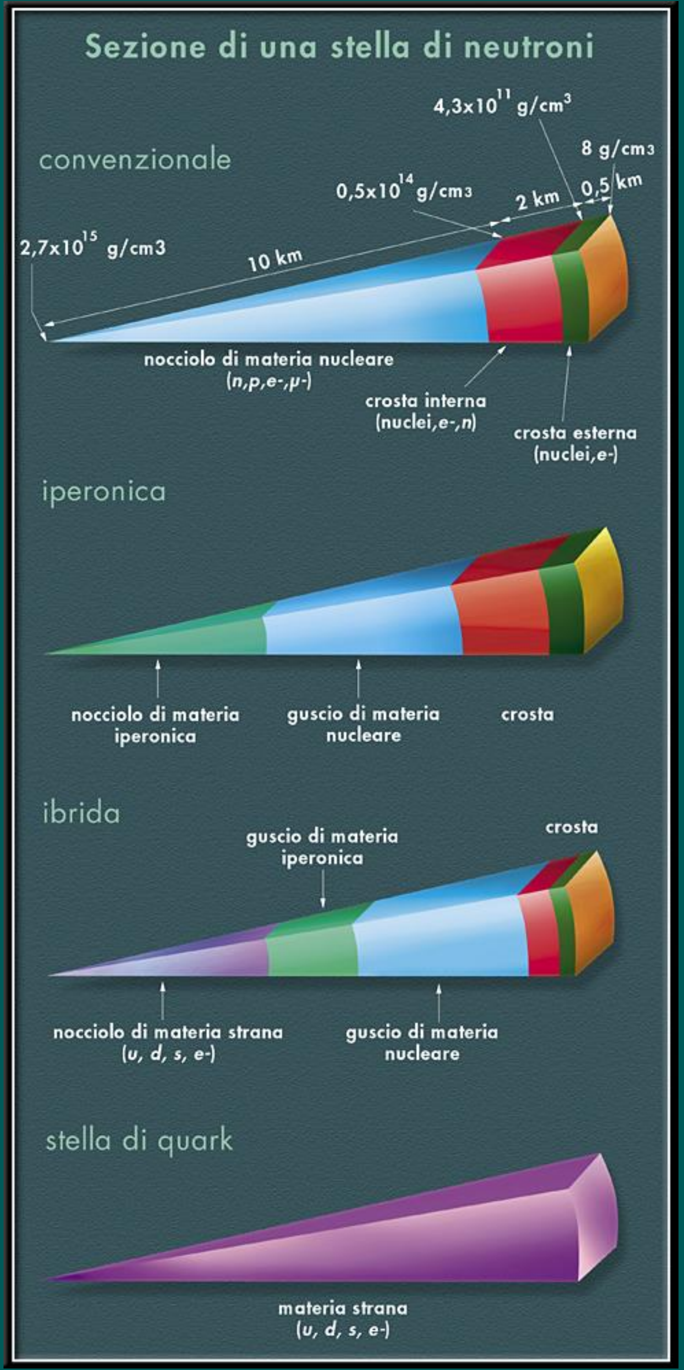

I. Bombaci, A. Drago, INFN Notizie, n. 13, 15 (2003)

Nucleon Stars

Hyperon Stars

Hybrid Stars

Strange Stars

EOS of nuclear matter and Neutron Stars
(Nucleon Stars)

β-stable nuclear matter

$$p + e^- \leftrightarrow n + \nu_e$$
$$\bar{\nu}_e + p \leftrightarrow n + e^+$$

$$\mu_e \geq m_\mu$$
$$e^- \rightarrow \mu^- + \nu_e + \bar{\nu}_\mu$$

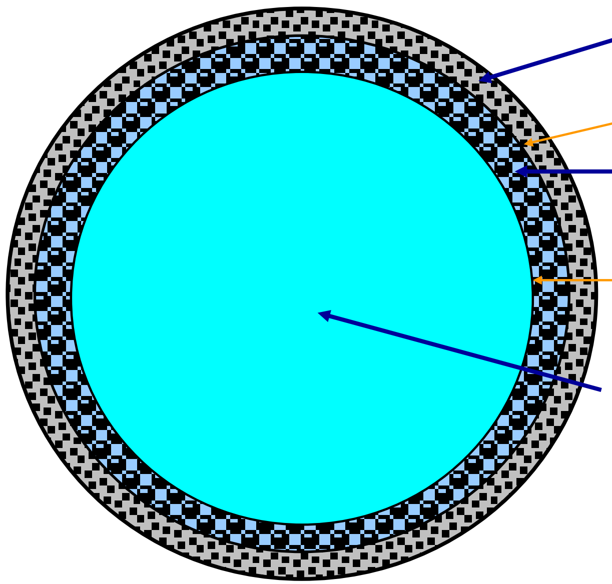

- **Equilibrium with respect to the weak interaction processes**

$$\mu_n - \mu_p = \mu_e$$
$$\mu_\mu = \mu_e$$

- **Charge neutrality**

$$n_p = n_e + n_\mu$$

neutrino-free matter

$$\mu_\nu = \mu_{\bar{\nu}} = 0$$

To be solved for any given value of the total baryon number density *n*

Microscopic approach to asymmetric nuclear matter EOS

input

Two-body nuclear interactions: V_{NN}

Parameters fitted to

NN scatering data with **χ^2/datum ~1**

Three-body nuclear interactions: V_{NNN}

Parameters fitted to

- **binding energy of A = 3, 4 nuclei** or
- **empirical saturation point of symmetric nuclear matter**:

$n_0 = (0.16 \pm 0.01)\ fm^{-3}$, $E/A = (-16 \pm 1)$ MeV

	AV18	AV18/UIX	Exp.
B(3H)	7.624	8.479	8.482
B(3He)	6.925	7.750	7.718
B(4He)	24.21	28.46	28.30

Values in MeV

Nuclear Matter at **$n = 0.16\ fm^{-3}$**

$E^{pot}(2BF)/A \sim$ - 40 MeV

$E^{pot}(3BF)/A \sim$ - 1 MeV

A new microscopic EOS model for nuclear matter

I. Bombaci, D. Logoteta, Astron. and Astrophys. 609 (2018) A128

Available in tabular form on **CompOSE** web site
https://compose.obspm.fr/eos/120/

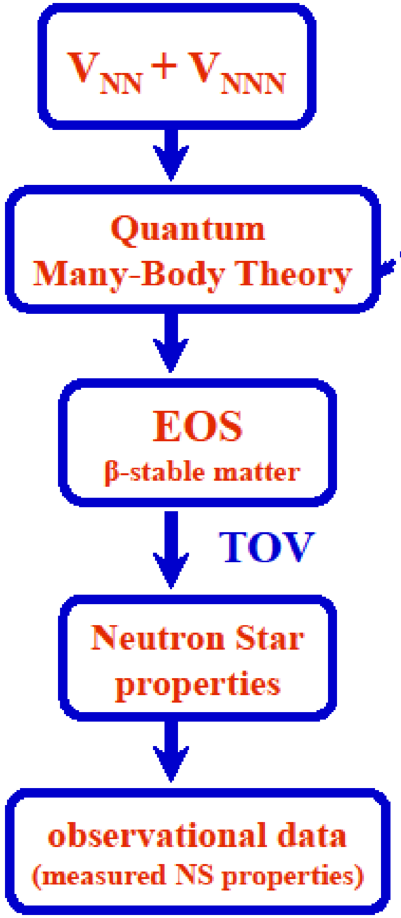

e.g.
Brueckner-Hartree-Fock
$V_{NN} \rightarrow G_{NN}$

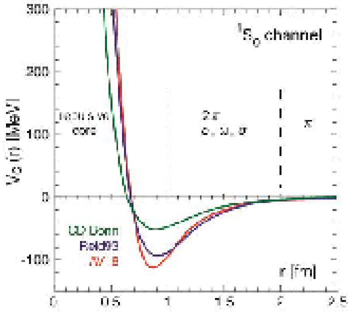

Interactions

NN ChEFT N3LO Δ(1232)
Piarulli et al., Phys. Rev. C 94 (2016) 054007

NNN ChEFT N2LO Δ(1232)
Epelbaum et al., Phys. Rev C 66 (2002) 064001
Navratil, Few-Body Syst. 41 (2007) 117
average → $V^{eff}_{NN}(n)$
Logoteta et al., Phys. Rev. C 94 (2016) 064001

Energy per nucleon (Symmetric NM)

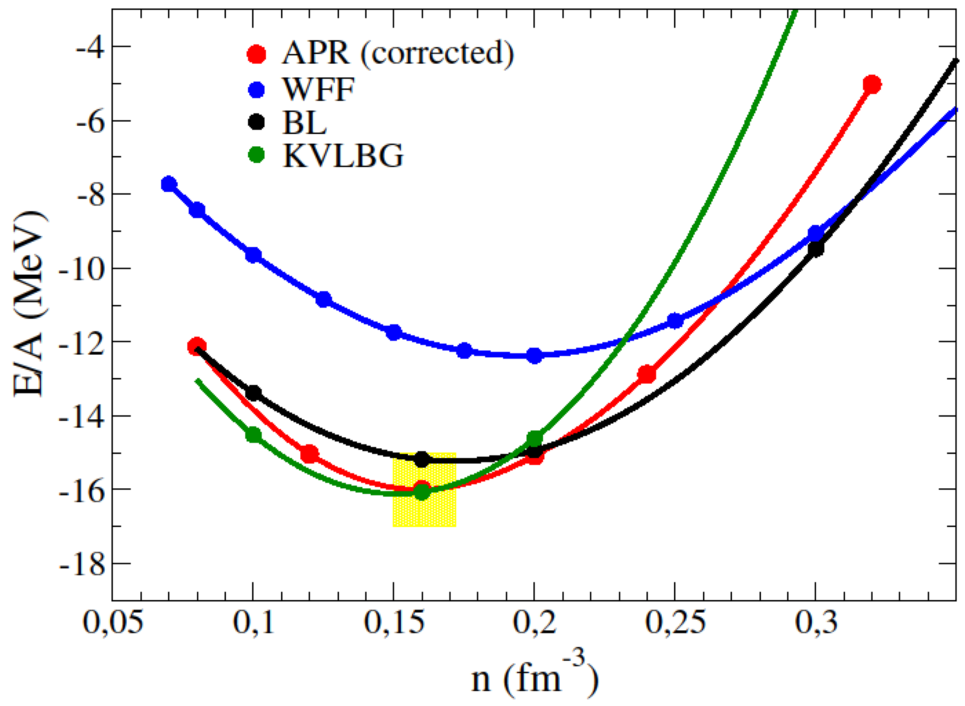

Nuclear matter properties at the saturation density

EOS	n_0 (fm^{-3})	E_0 (MeV)	E_{sym} (MeV)	L (MeV)	K_0 (MeV)
BL	**0.17**	**-15.2**	**35.4**	**76.0**	**190**
KVLBG	**0.15**	**-16.1**	**35.2**	**70.2**	**251**
WFF	**0.19**	**-12.4**	**31.0**	**56.5**	**209**
APR	**0.16**	**-16.0**	**33.9**	**59.4**	**266**
APR_{micro}	**0.18**	**-12.4**	**32.8**	**69.4**	**----**
empirical	**0.16 ± 0.01**	**-16 ± 1**	**25 – 37**	**30 – 90**	**180 – 260**

BL : I. Bombaci, D. Logoteta, Astron. and Astrophys. 609 (2018) A128

WFF : R.B. Wiringa, V. Ficks and A. Fabrocini, Phys. Rev. C **38** (1988) 1010.

APR :A. Akmal, V.R. Pandharipande and D.G. Ravenhall, Phys. Rev. C **58** (1998) 1804.

KVLBG :A. Kievsky, M. Viviani, D. Logoteta, I. Bombaci and L. Girlanda, Phys. Rev. Lett. **121** (2018) 072701.

Selecting Nuclear Matter EOS: basic requirements

Nuclear Symmetry Energy

$$E_{sym}(n) = E_{sym}(n_0) + L \left(\frac{n-n_0}{3n_0}\right) + \frac{1}{2!} K_{sym} \left(\frac{n-n_0}{3n_0}\right)^2 + \frac{1}{3!} Q_{sym} \left(\frac{n-n_0}{3n_0}\right)^3 + \cdots$$

Symmetry energy **slope parameter** $L = 3n_0 \left.\frac{\partial E_{sym}(n)}{\partial n}\right|_{n_0}$

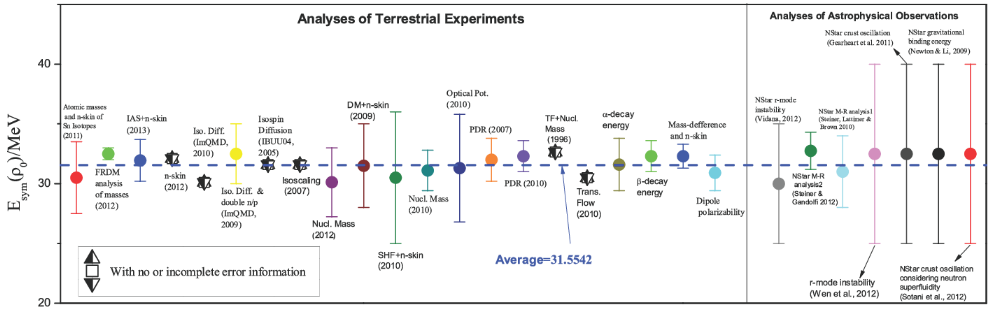

$E_{sym}(n_0) = (25 – 37)$ MeV

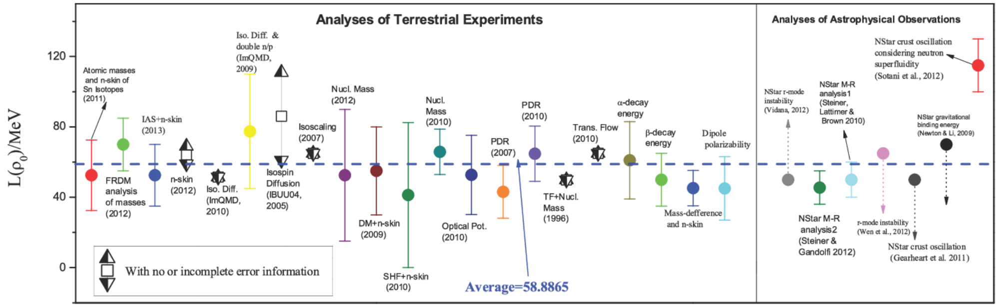

L = (30 – 90) MeV

From various **nuclear physics experimental data**: **B.A. Li and X. Han, Phys. Lett. B 727 (2013) 276**

Neutron Skin Thickness: the PREX-II experiment

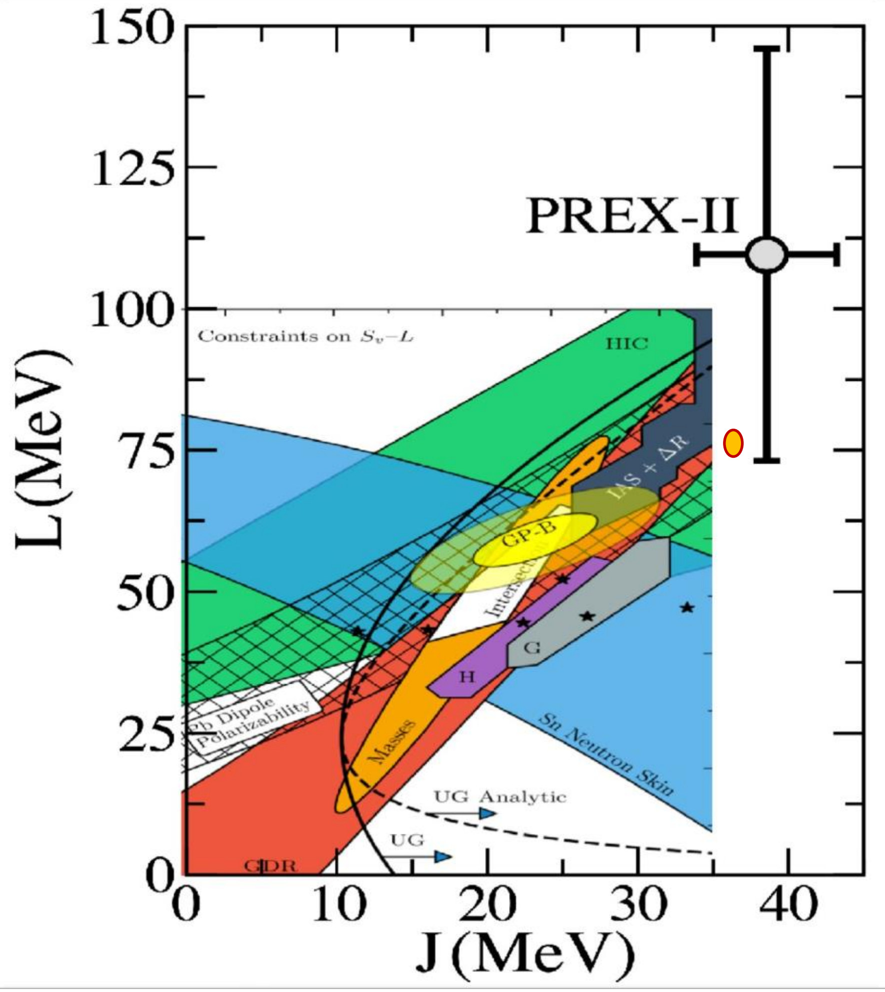

Accurate measurements of the neutron skin thickness Δr_{np} in neutron rich nuclei via **parity-violating electron scattering** at JLab can constrain the **symmetry energy $E_{sym}(n_0) \equiv J$** at the saturation density and **its slope parameter L.**

D. Adhikari et al. (PREX Collaboration), Phys. Rev. Lett. 126 (2021).

$$\Delta r_{np}(^{208}Pb) = 0.283 \pm 0.071\ fm$$

$E_{sym}(n_0) \equiv J$ = 33.4 – 42.8 MeV

L = 69 – 143 MeV

BL EOS: $E_{sym}(n_0)$ = 35.4 MeV, L = 76.0 MeV

For asymmetric Nuclear Matter as a mixture of neutrons and protons free Fermi gases $L = 2E_{sym}(n_0)$

Symmetry energy

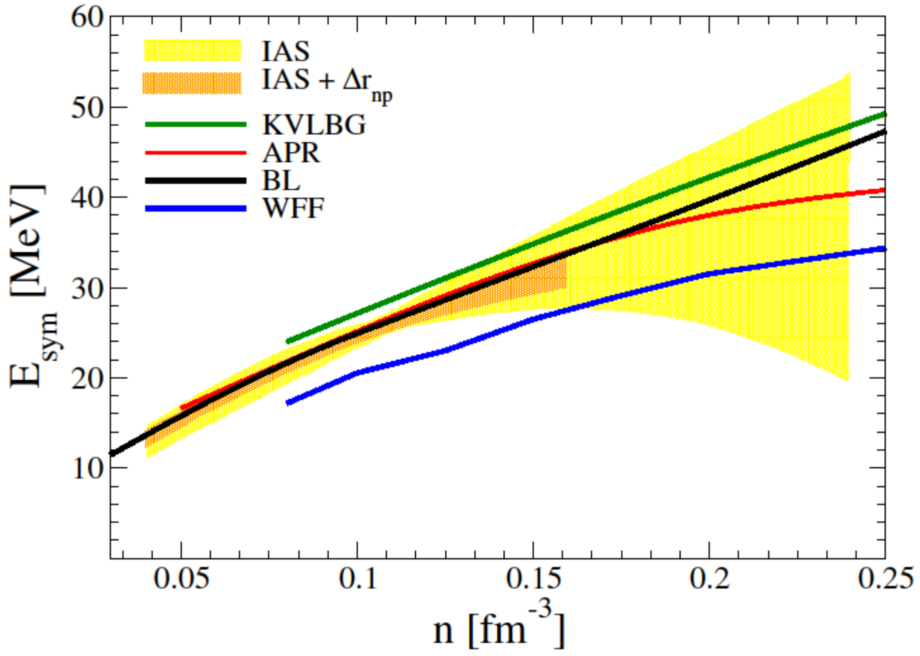

IAS = constraint from Isobaric Analog States in nuclei
(P. Danielewicz, J. Lee, Nucl. Phys. A922 (2014) 1)
Δr_{np} = neutron skin thickness of heavy nuclei
(X. Roca-Maza et al., Phys. Rev. C 87 (2013) 034301)

Particle fractions

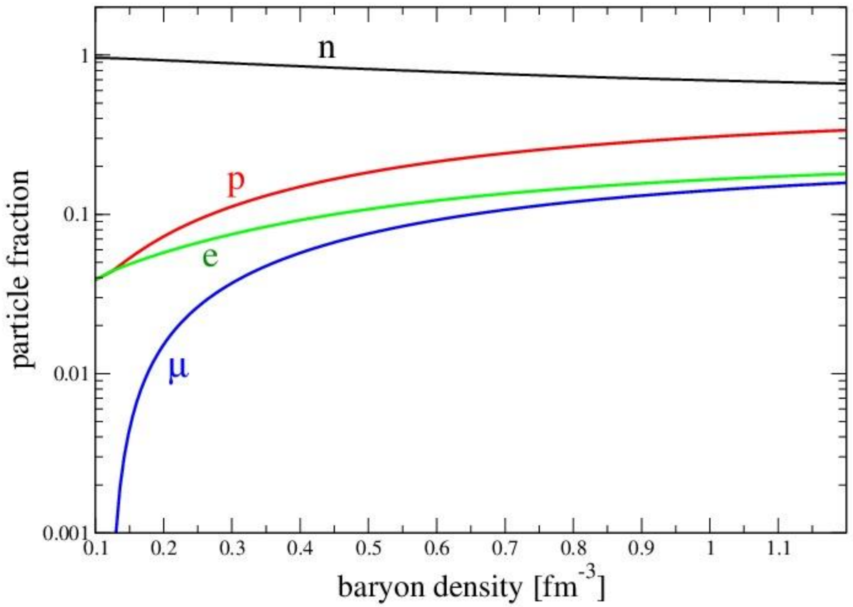

Pressure in symmetric NM

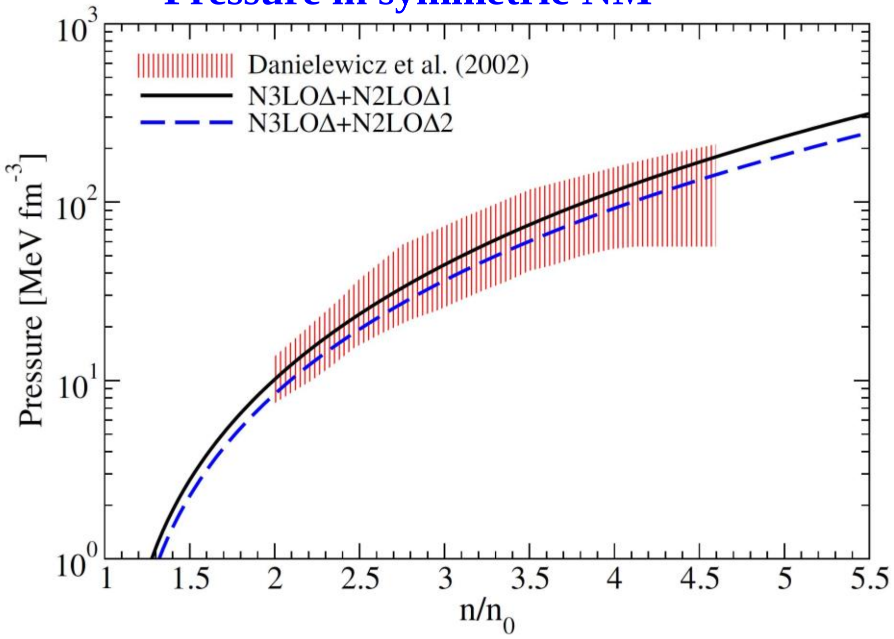

The red hatched area represents the region in the pressure–density plane for **SNM** which is consistent with the measured **elliptic flow of matter in collision experiments between heavy atomic nuclei** (Danielewicz et al. 2002).

I. Bombaci, D. Logoteta, Astron. and Astrophys. 609 (2018) A128

Dependence of the nuclear EOS on the quantum many-body approach

Benchmark calculations of pure neutron matter with realistic nuclear interactions

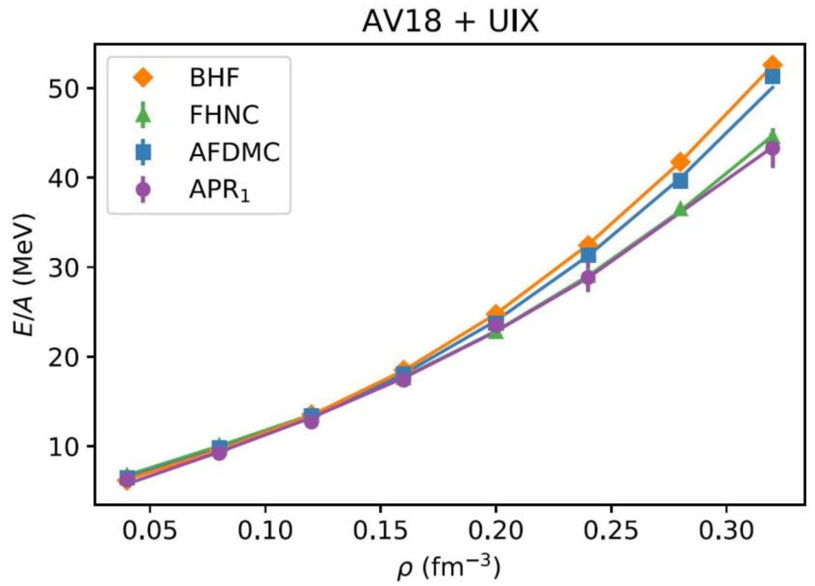

Brueckner-Hartree-Fock (BHF)

Fermi hypernetted chain/ single-operator chain (FHNC)

auxiliary-field diffusion Monte Carlo (AFDMC)

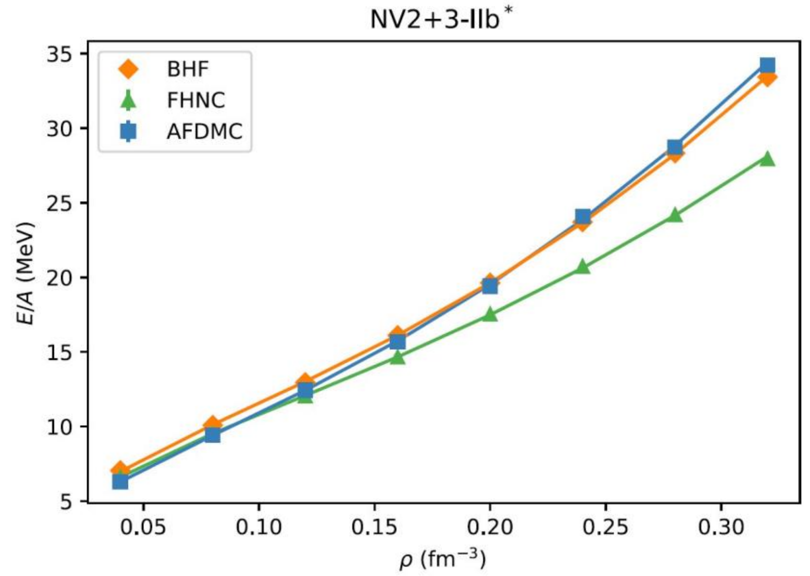

M. Piarulli, I. Bombaci, D. Logoteta, A. Lovato, R.B. Wiringa, Phys. Rev. C 101 (2020)
A. Lovato, I. Bombaci, D. Logoteta, M. Piarulli, R.B. Wiringa, Phys. Rev. C 105 (2022)

Neutron Stars

mass-radius relation

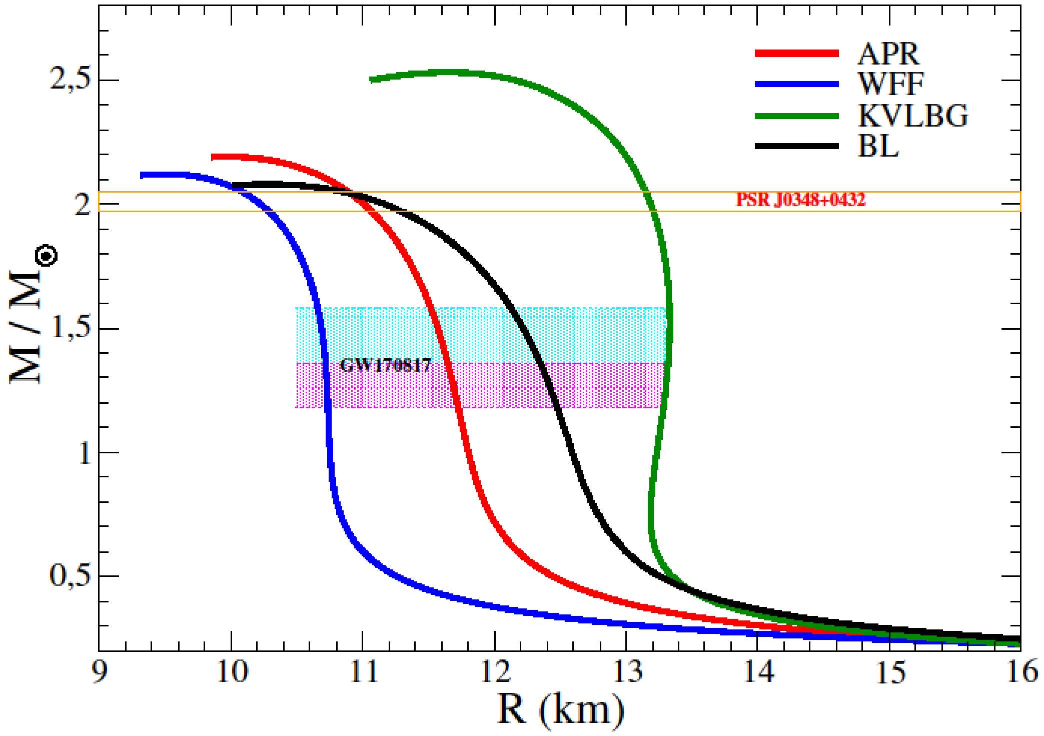

Properties of the Maximum mass configuration

EOS	n_c (fm^{-3})	n_c / n_0	ρ_c (10^{14} g/cm ^{3})	M ($M_\odot$)	R (km)
BL	1.156	7.23	27.37	2.08	10.28
KVLBG	0.845	5.28	20.25	2.53	11.65
WFF	1.247	7.79	30.12	2.12	9.50
APR	1.146	7.16	27.87	2.19	9.97

GW170817 data from: **B. P. Abbot et al. (LIGO-Virgo collaboration), Phys. Rev. Lett. 119 (2017) 161101**

$R_1 = (11.9 \pm 1.4)$ km and **$R_2 = (11.9 \pm 1.4)$ km** for the radius of the two neutron stars and **$1.36 \leq M_1 / M_\odot \leq 1.58$** and **$1.18 \leq M_2 / M_\odot \leq 1.36$** for their masses at the 90% credible level, for the case of "low-spin" prior.

NICER: Neutron Star Interior Composition Explorer

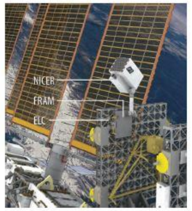

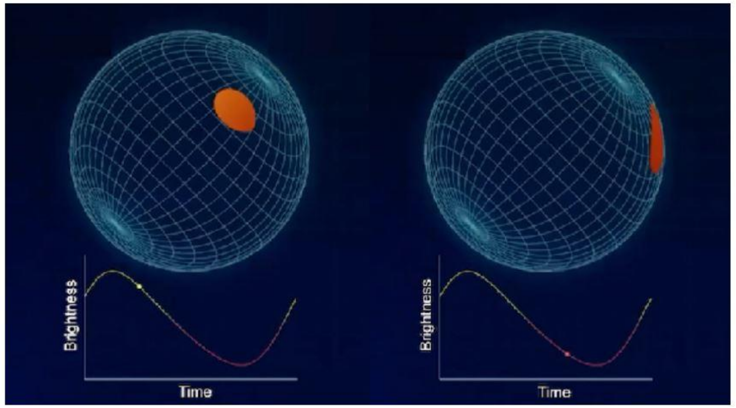

A new way of measuring NS radius by tracking the X-ray emission from “hot spots” on the star’s surface as the star rotates. M/R is extracted by modeling the Pulse Profile of the hot spots

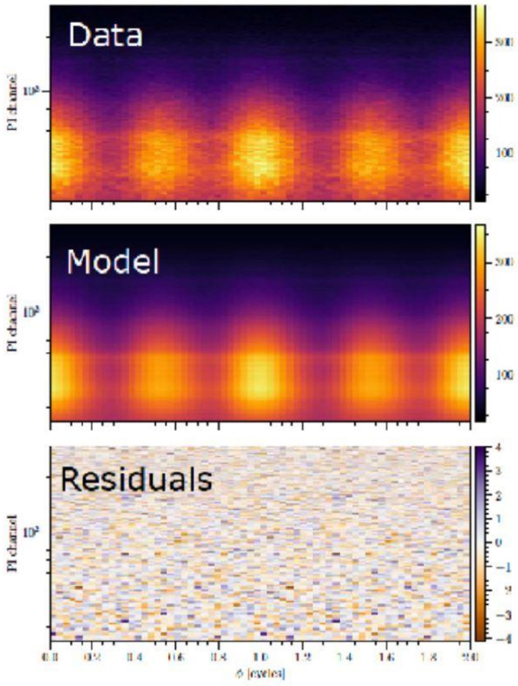

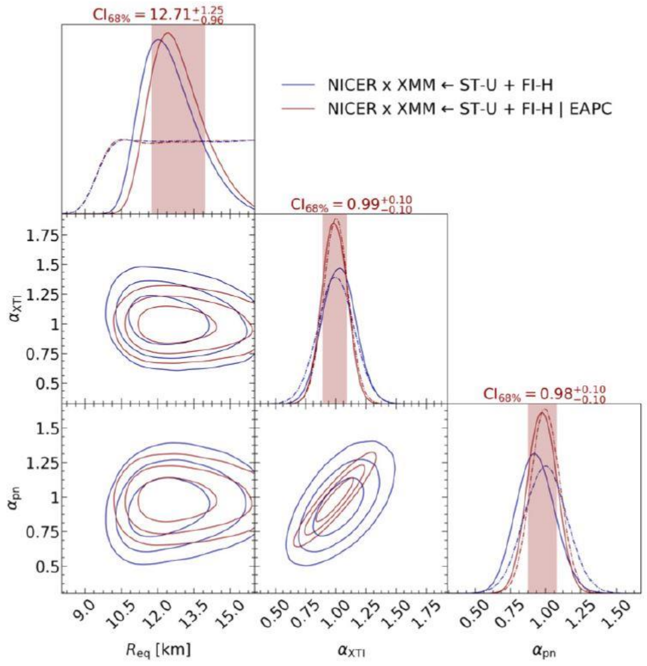

✧ PSR J0740+6620

$M = 2.072^{+0.067}_{-0.066} M_\odot$

$R = 13.7^{+2.6}_{-1.5}$ km Miller et al., arXiv:2105.06979

$R = 12.39^{+1.30}_{-0.98}$ km Riley et al., arXiv:2105.06980

✧ PSR J0030+0451

$M/R = 0.156^{+0.008}_{-0.010}$

$R = 13.02^{+1.24}_{-1.06}$ km Miller et al., ApJ 887 L24 (2019)

$R = 12.71^{+1.14}_{-1.19}$ km Riley et al., APJ 887 L21 (2019)

Slide by Isaac Vidana

Constraints from astrophysical observations

PSR J0740+6620

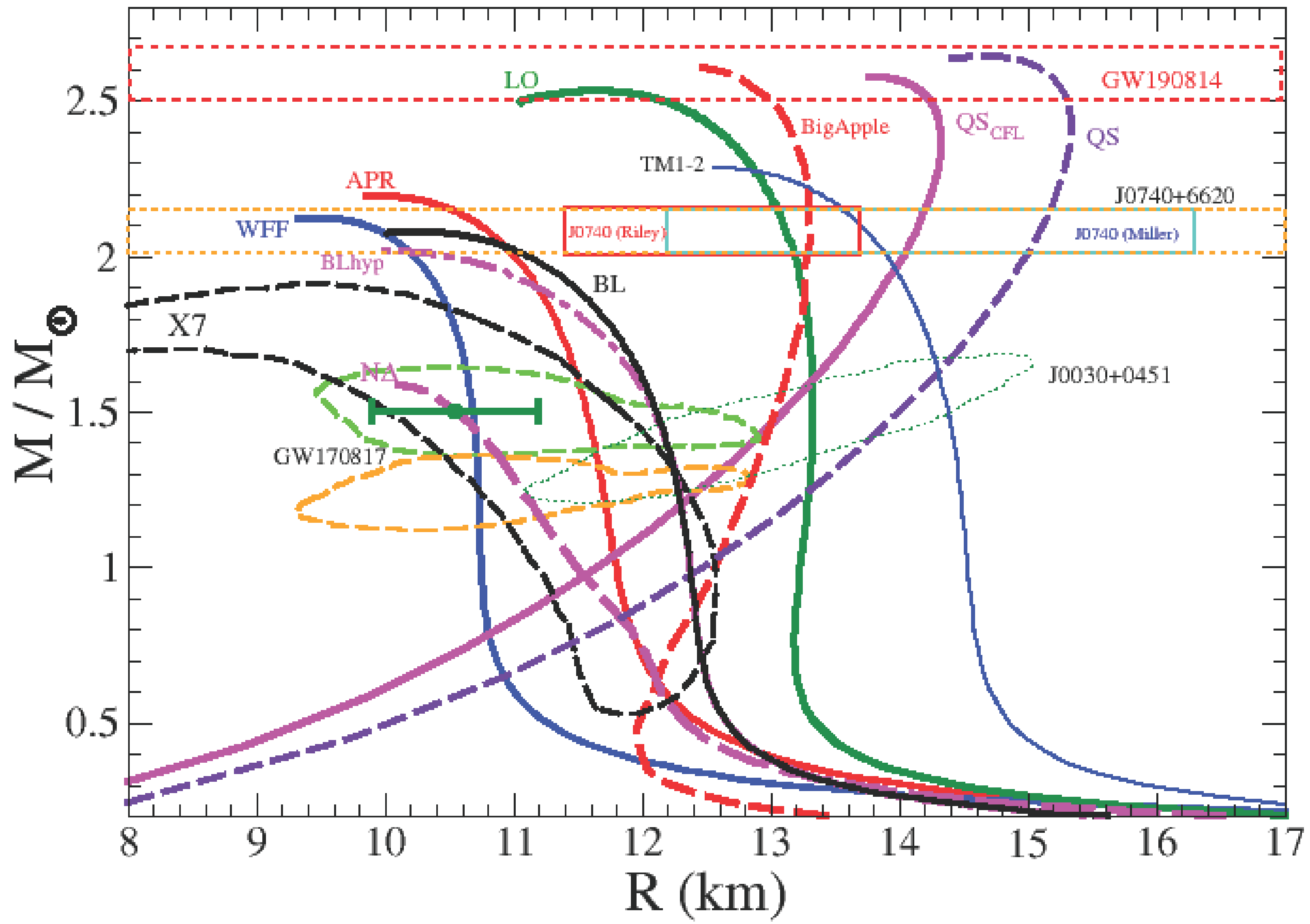

NICER data

T.E. Riley et al. (2021) arXiv:2105:06980

M.C. Miller et al. (2021) arXiv:2105:06979

GW190814

In August 2019, the LIGO-Virgo gravitational-wave network observed a GW signal produced by the merger of a **23 $M_\odot$ black hole** and a **compact star with mass $M_2 = (2.50 – 2.67)\ M_\odot$**.

GW190814's secondary mass lies in the hypothesized lower **mass gap of 2.5–5 $M_\odot$ between known NSs and BHs.**

GW190814's secondary could be the **heaviest neutron star** or the **lightest black hole** ever observed.

R. Abbott et al., Astrophys. J. Lett. 896 (2020) L44

or could GW190814's secondary be a **Strange Quark Star?**

I. Bombaci, A. Drago, D. Logoteta, G. Pagliara, I. Vidaña, Phys. Rev. Lett. 126 (2021) 162702

Two coexisting families of Compact Stars

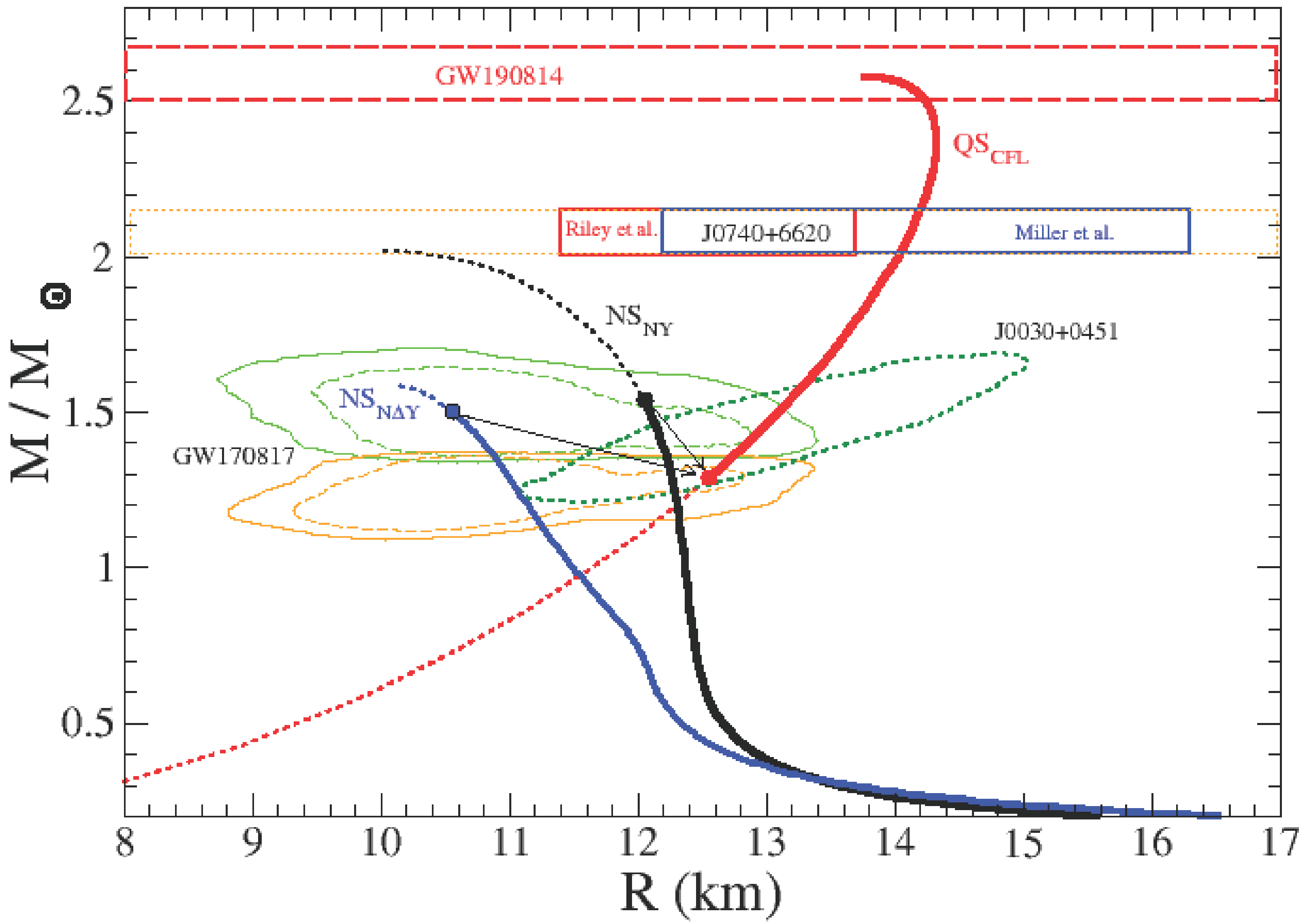

consistent with the interpretation of the secondary component of GW190814 as a strange quark star

and

relieve the tension between some measurements of NS radii

(stars with «small» radii are Hadroic Stars and stars with «large» radii are Strange Quark Stars)

I. Bombaci, A. Drago, D. Logoteta, G. Pagliara, I. Vidaña, Phys. Rev. Lett. 126 (2021) 162702

Two coexisting families of Compact Stars

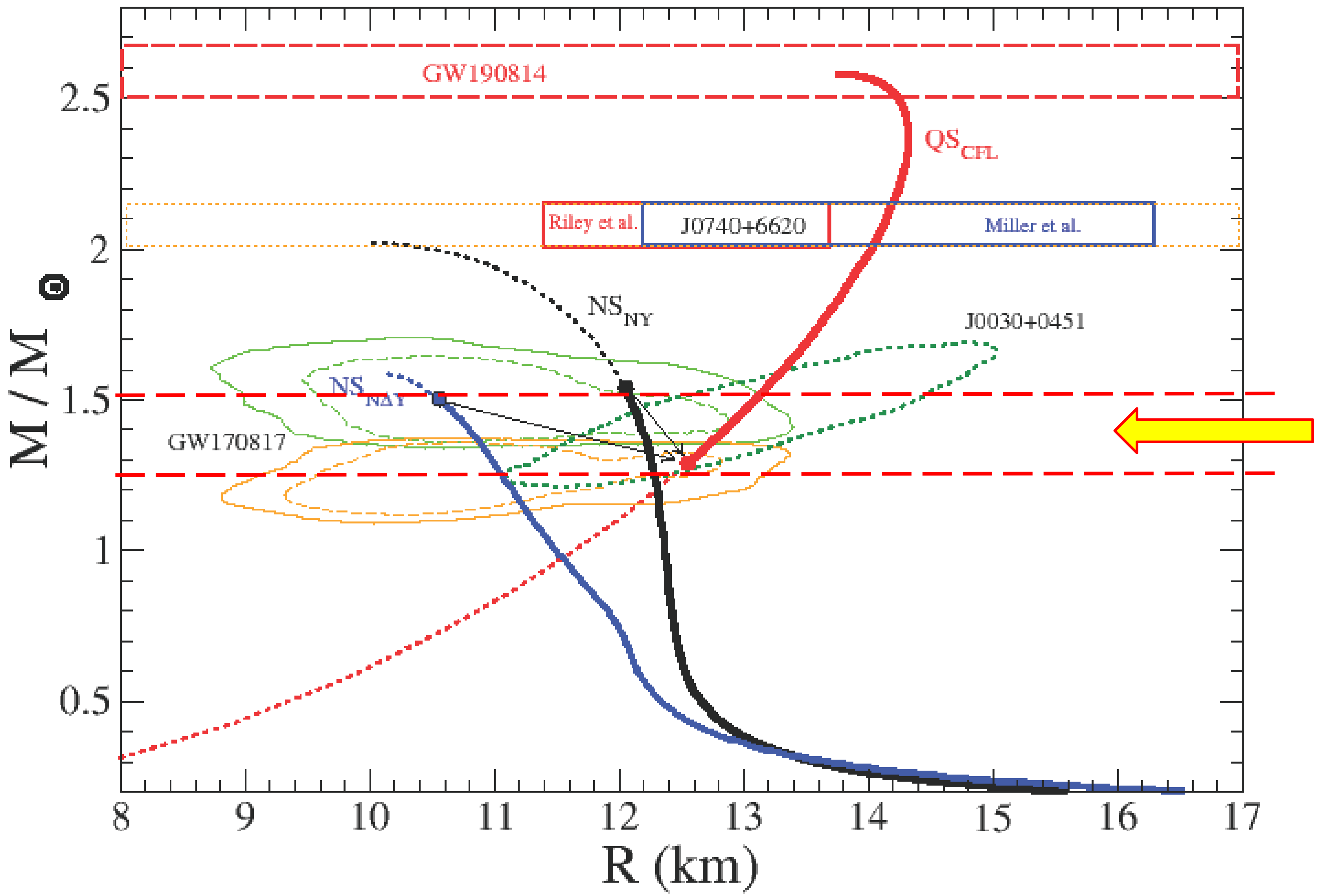

An observationally testable prediction of the two-family scenario:

existence in nature of compact stars having the same mass but different radii.

This observation would falsify the scenario with a single family of compac stars (hadronic stars).

I. Bombaci, A. Drago, D. Logoteta, G. Pagliara, I. Vidaña, Phys. Rev. Lett. 126 (2021) 162702

HESS J1731-347: a neutron star with an unusually small mass

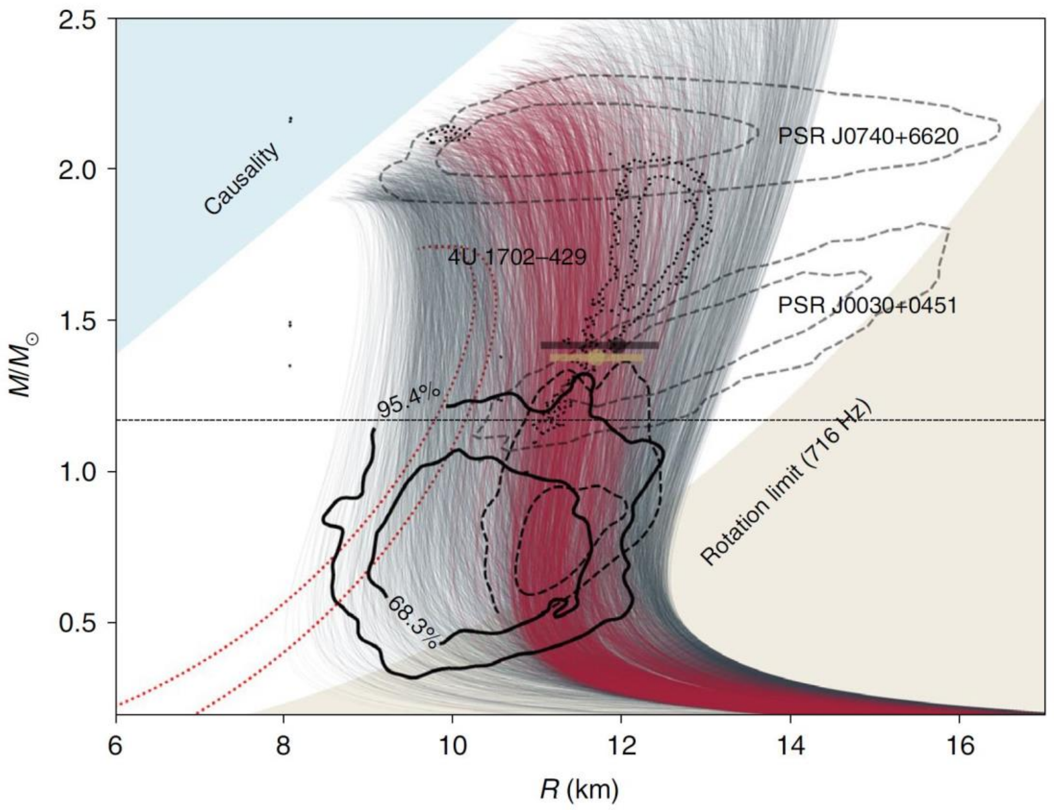

Central Compact Objeect in
the Supernova Remnant HESSE J1731-347

$$M = 0.77^{+0.20}_{-0.17}\ M_{\odot}$$

$$R = 10.4^{+0.86}_{-0.78}\ km$$

V. Doroshenko et al., Nature Astronomy 6, 1444 (2022)

HESS J1731-347: a neutron star with an unusually small mass

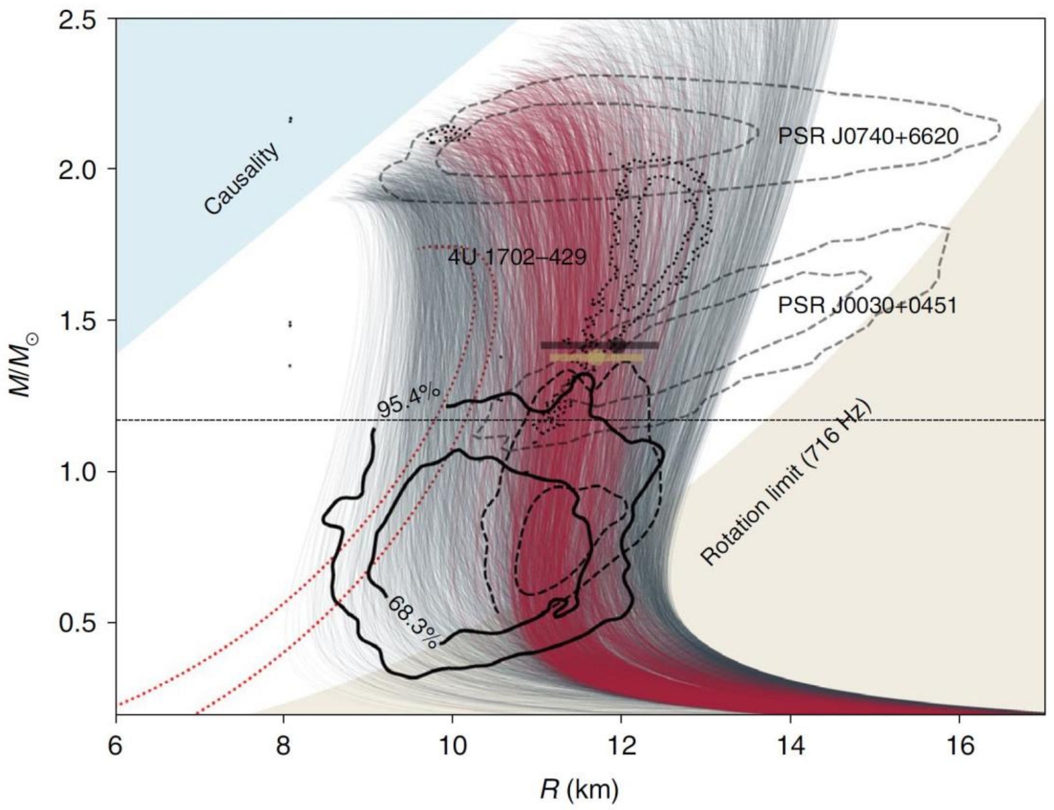

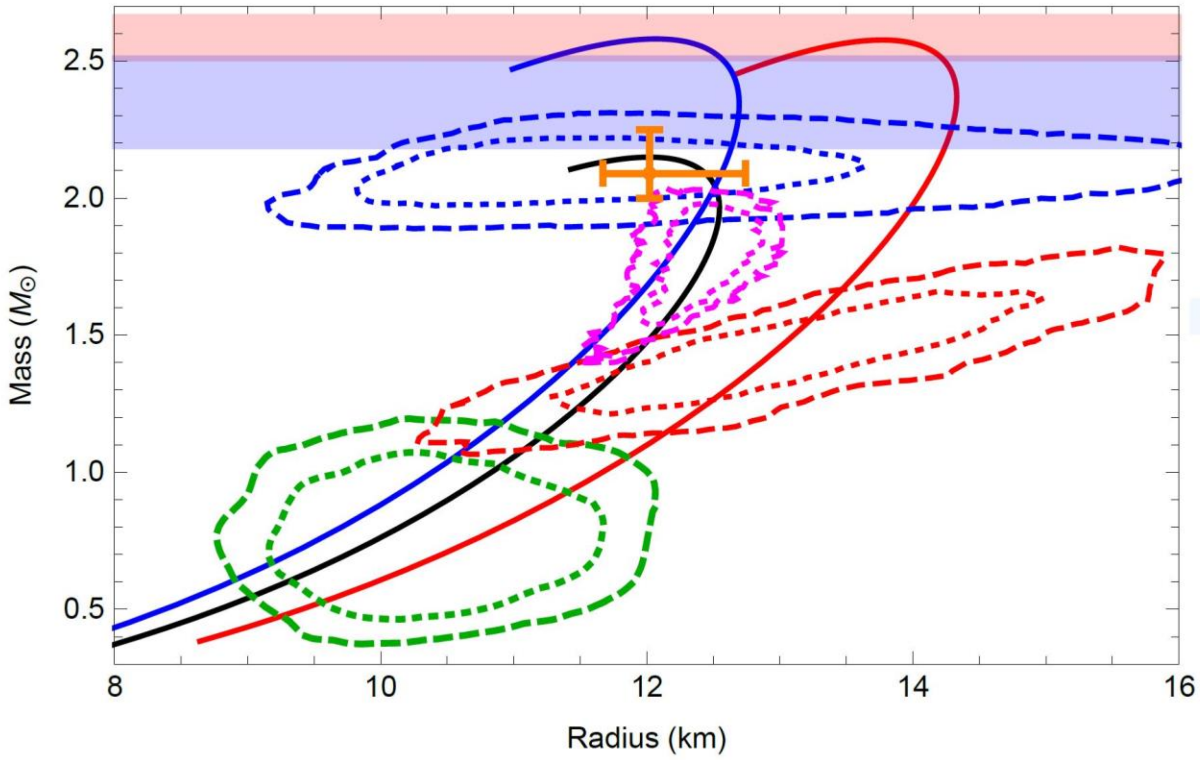

Is the compact object associated with HESSE J1731-347 a strange quark star?

F. Di Clemente, A. Drago, G. Pagliara,
arXiv:2211.07485 (Nov. 2022)

Message taken from **Nucleon Stars**

(i.e. Neutron Stars with a pure nuclear matter core)

NN interactions are essential to have “large” stellar mass

For a free neutron gas $M_{max} = 0.71\ M_{\odot}$ **(Oppenheimer and Volkoff, 1939)**

NNN interactions are essential

(i) to reproduce the correct **empirical saturation point of nuclear matter**

(ii) to reproduce measured neutron star masses, i.e. to have $M_{max} > 2\ M_{\odot}$

models of Nucleon Stars

(i.e. Neutron Stars with a pure nuclear matter core)

are able to explain measured Neutron Star masses
as those of

PSR J1614-2230, PSR J0348+0432 and PSR J0740+6620

$$M_{NS} \approx 2\, M_{\odot}$$

Happy?

Not the end of the story!

The EOS of Nuclear Matter at finite temperature

Extension of the BHF approximation a T ≠ 0

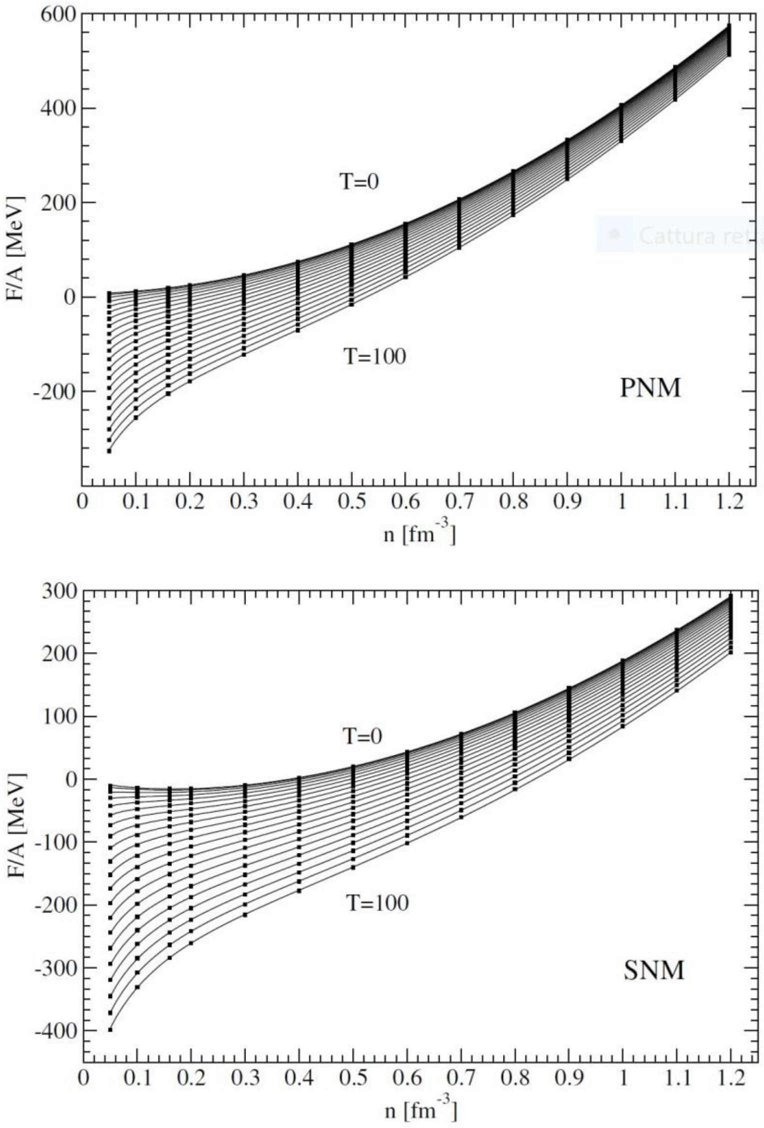

Free energy per particle F/A

D. Logoteta, A. Perego, I. Bombaci, Astron. & Astrophys. 646 (2021)

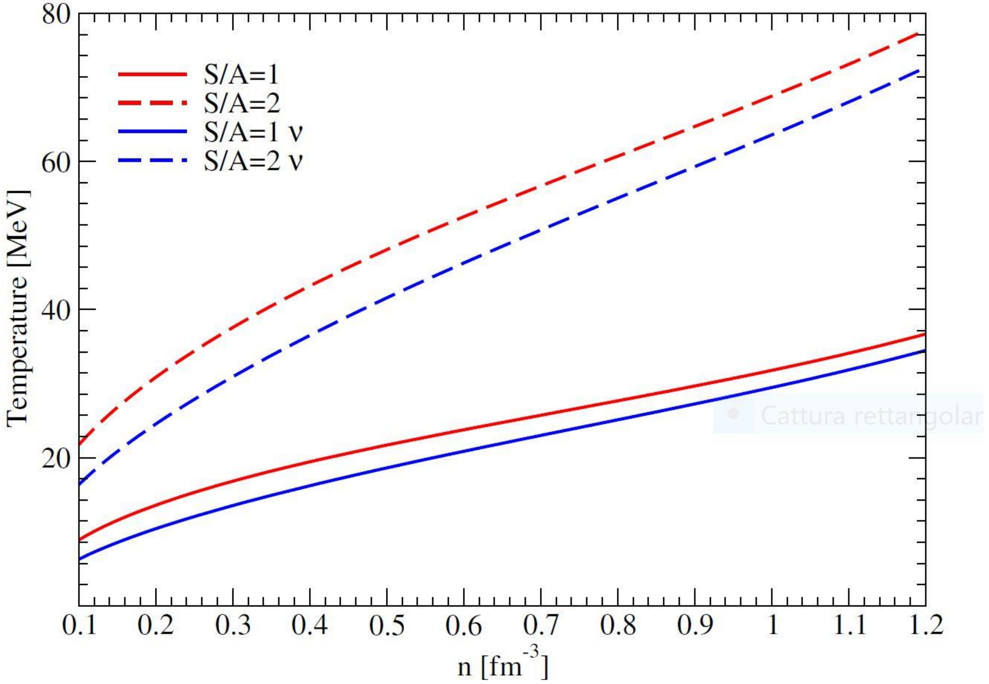

Fig. 5. Temperature profiles as a function of nuclear density n for isoentropic ($S/A = \mathrm{const}$) β-stable EOSs in the case of neutrino-free (red lines) and neutrino trapped (blue lines) matter.

$$T_S = \chi(\beta)\,\frac{S}{A}\,n^{2/3}\,,$$

where

$$\chi(\beta) = \frac{\hbar^2}{m}\left(\frac{3}{\pi}\right)^{2/3}\left[\left(\frac{1+\beta}{2}\right)^{1/3} + \left(\frac{1-\beta}{2}\right)^{1/3}\right]^{-1}.$$

I. Bombaci, T.T.S. Kuo, U. Lombardo, Phys. Rep. 242 ((1994)

Hyperons in dense matter and Hyperon Stars

Strange baryons: the **baryon octet : J^{π} = (1/2)$^+$**

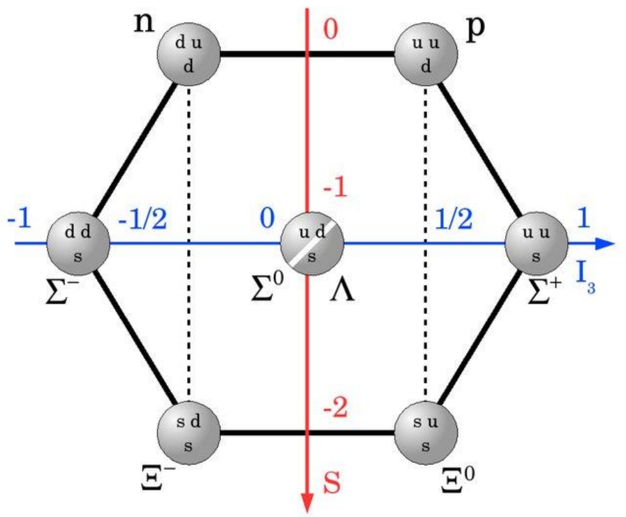

baryon name	Isospin	I_3	S	quarks	mass (MeV/c^2)	mean life
n	1/2	-1/2	0	udd	939.56	880 s
p	1/2	+1/2	0	uud	938.27	stable
Λ	0	0	-1	uds	1115.68	2.63×10^{-10} s
Σ^-	1	-1	-1	dds	1197.43	1.48×10^{-10} s
Σ^0	1	0	-1	uds	1192.55	7.4×10^{-20} s†
Σ^+	1	+1	-1	uus	1189.37	0.80×10^{-10} s
Ξ^-	1/2	-1/2	-2	dss	1321.32	1.64×10^{-10} s
Ξ^0	1/2	+1/2	-2	uss	1314.90	2.90×10^{-10} s

† The Σ^0 decays via the electromagnetic process $\Sigma^0 \rightarrow \Lambda + \gamma$ followed by the weak decay of the Λ.

Hypernuclei: (n, p, Y) bound states

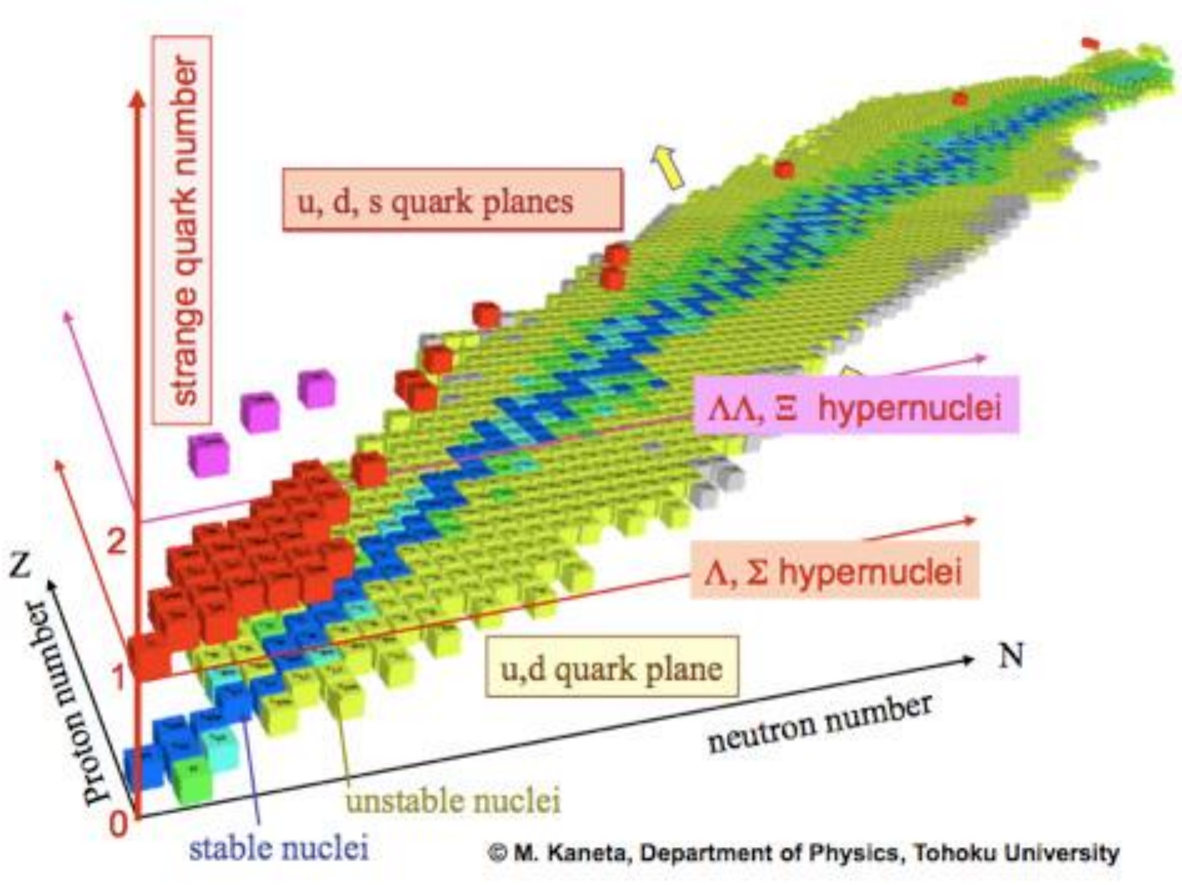

valuable informations on the interactions between nucleons and hyperons

Hyperons formation in dense nuclear matter

$$p + e^- \rightarrow \Lambda + \nu_e$$
$$n + e^- \rightarrow \Sigma^- + \nu_e$$

etc.

$$\mu_p = \mu_n - \mu_e = \mu_{\Sigma^+}$$

$$\mu_n = \mu_{\Sigma^0} = \mu_{\Xi^0} = \mu_\Lambda$$

$$\mu_n + \mu_e = \mu_{\Sigma^-} = \mu_{\Xi^-}$$

$$\mu_\mu = \mu_e$$

$$n_p + n_{\Sigma^+} = n_e + n_\mu + n_{\Sigma^-} + n_{\Xi^-}$$

(neutrino-free matter)

At sufficiently high density nuclear matter turns into hyperonic matter

Hyperons threshold densities

(1) a simple extimate: **{n,p,e⁻} ideal gas in β-equilibrium** (**no strong interaction**) [non-rel. (n, p), ultrarel. e⁻]

$$\mu_n = \mu_p + \mu_e = m_\Lambda c^2 \longrightarrow n^{*\Lambda} = 0.86\, fm^{-3} = 5.4\, n_0$$

(2) Effect of the **strong interaction**

NN(Av18) + NNN + NY(ESC08b)
(no hyperonic TBF)

$$n^{*\Lambda} = 0.35\, fm^{-3} = 2.19\, n_0$$

$$n^{*\Sigma^-} = 0.64\, fm^{-3} = 4\, n_0$$

$$n^{*\Lambda}, n^{*\Sigma^-} < n_c(M_{max})$$

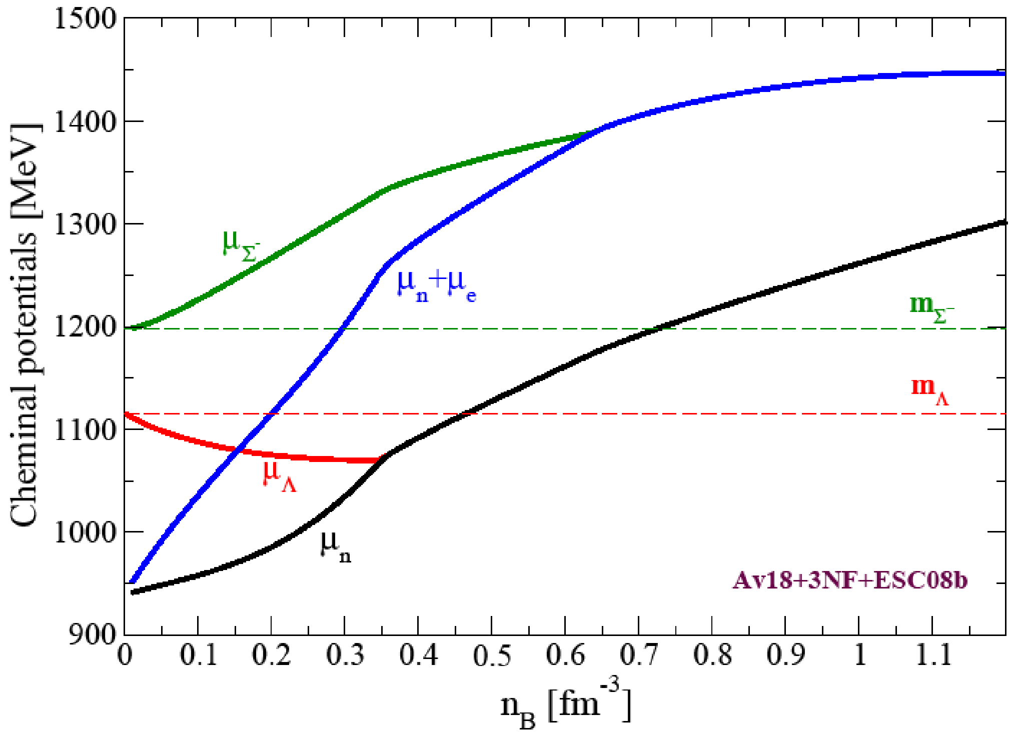

I. Bombaci, D. Logoteta, EPJ Web of Conference 117 (2016) 07005

Neutron stars: the maximum mass configuration

EOS	n_c (fm^{-3})	n_c / n_0	ρ_c (10^{14} g/cm ^{3})	M ($M_\odot$)	R (km)
BL	1.156	7.23	27.37	2.08	10.28
KVLBG	0.845	5.28	20.25	2.53	11.65
WFF	1.247	7.79	30.12	2.12	9.50
APR	1.146	7.16	27.87	2.19	9.97

I. Bombaci, D. Logoteta, Astron. and Astrophys. 609 (2018) A128

A. Kievsky, M. Viviani, D. Logoteta, I. Bombaci and L. Girlanda, Phys. Rev. Lett. **121** (2018) 072701

R.B. Wiringa, V. Ficks and A. Fabrocini, Phys. Rev. C **38** (1988) 1010.

A. Akmal, V.R. Pandharipande and D.G. Ravenhall, Phys. Rev. C 58 (1998) 1804.

Particle fractions

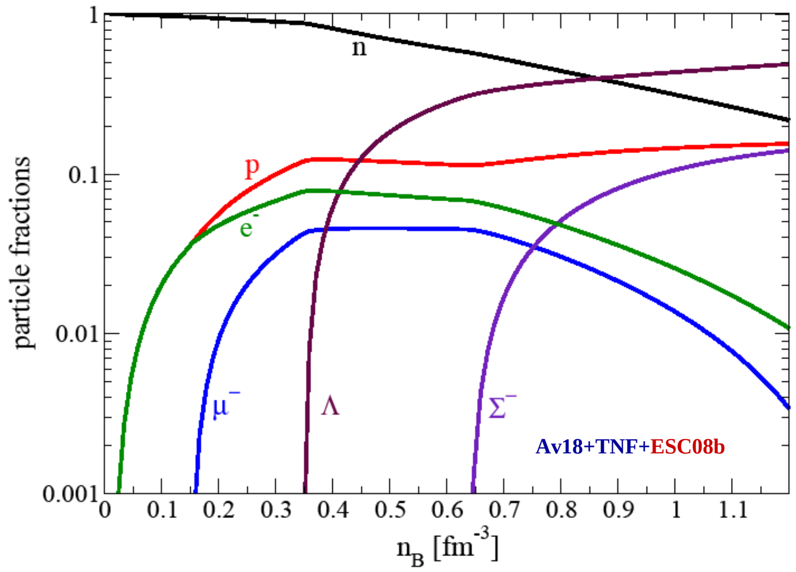

Equation of State of Hyperonic Matter

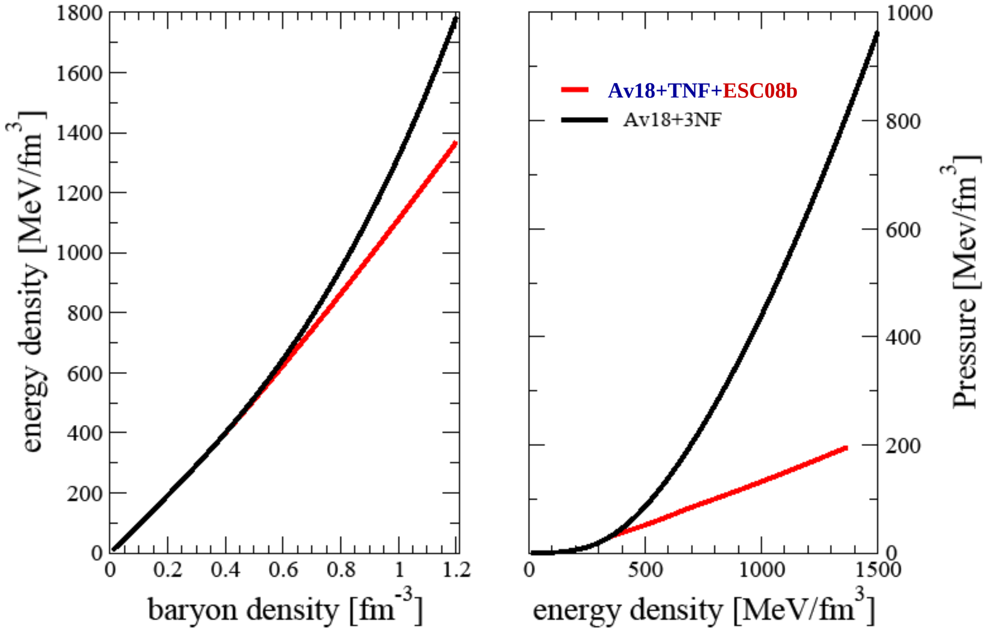

NN(Av18) + NNN + NY(ESC08b)

no hyperonic TBF

hyperons produce a strong softening of the EOS

Stellar mass

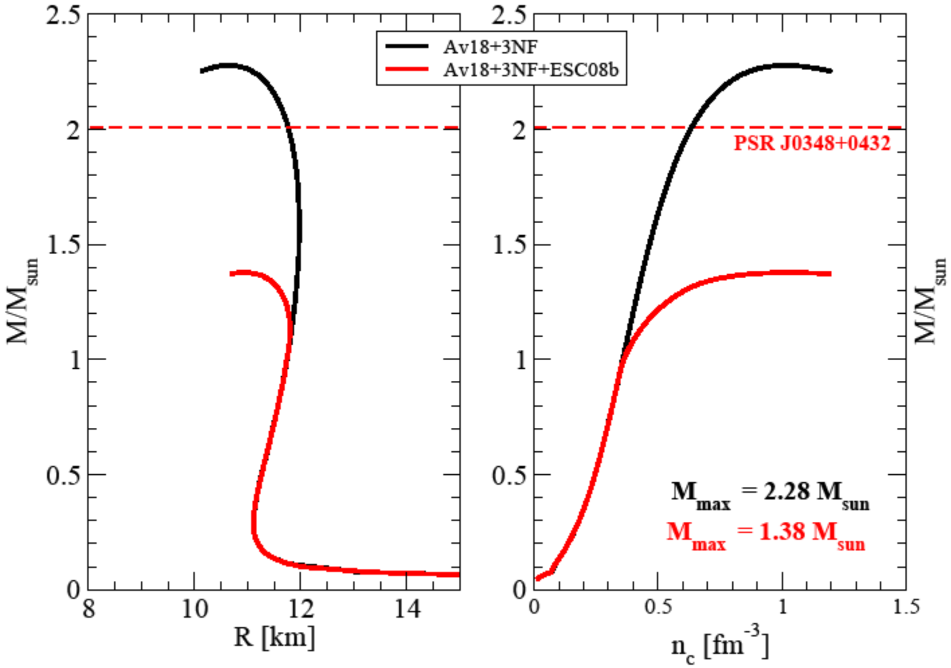

I. Bombaci, D. Logoteta, EPJ Web of Conference 117 (2016) 07005

Effect of the YY interaction

NN(Av18) + NNN + NY(ESC08 or NSC89)

no YY int.   no hyperonic TBF

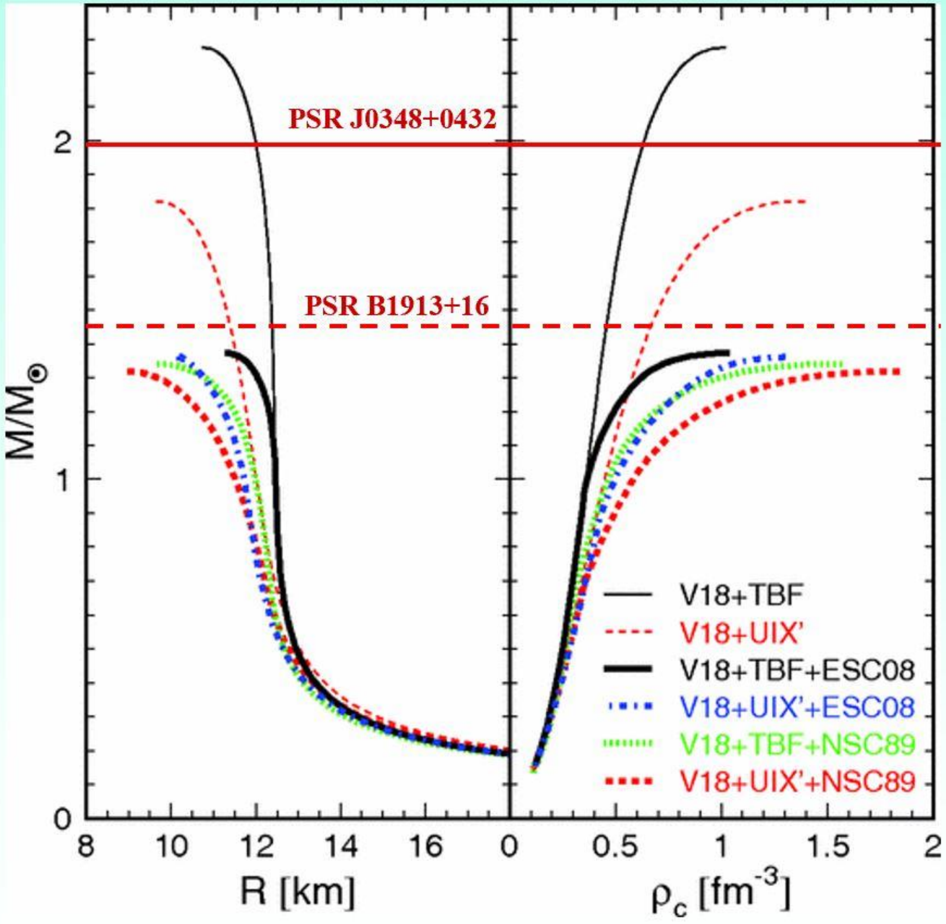

H.-J. Schulze, T. Rijken, Phys. Rev. C 84 (2011) 035801

NN(Av18) + NNN + NY + YY (ESC08c)

no hyperonic TBF

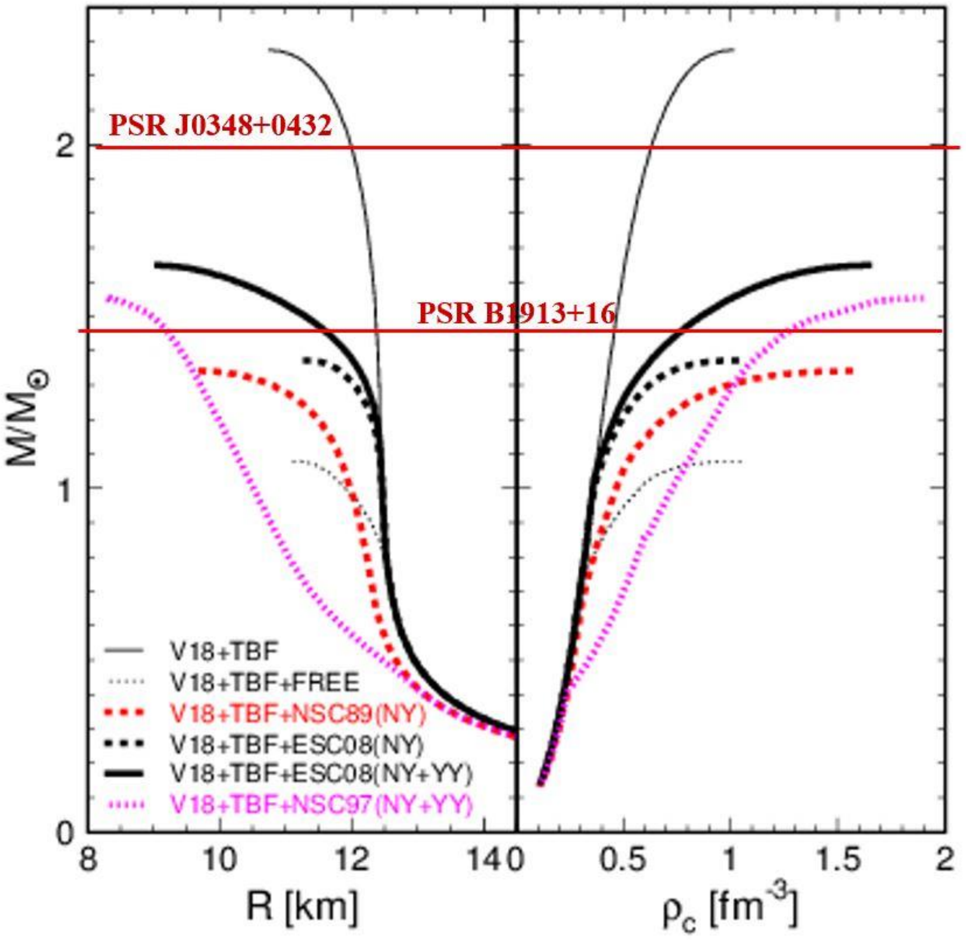

T. Rijken, H.-J. Schulze, Eur. Phys. J. A 52 (2016) 21

The hyperon puzzle in Neutron Stars

Many hyperonic matter EOS models (mostly microscopic models) **predict the presence of hyperons in the NS core, but they give**

$$M_{max} < 2\,M_{\odot}$$

not compatible with measured NS masses

A problem which likely originates from our incomplete knowledge of the baryonic interactions.

Hyperonic three-body interactions as a possible solution of the hyperon puzzle

As mentioned before, **three-nucleon interactions** are a necessary ingredient for an accurate description of nuclei and nuclear matter within non-relativistic approaches.

Thus, it is rather obvious to suppose the existence of **hyperonic three-body interactions** (of the type **NNY, NYY, YYY**).

The **NNΛ interaction** was in fact first hypothesized at the end of the 1950s (*), *i.e.* during the early days of hypernuclear physics, as an important ingredient to calculate the **binding energy of hypernuclei**.

It is thus reasonable to expect that **hyperonic three-body interactions** can influence dense-matter EoS and represent a **likely candidate to solve the hyperon puzzle**.

(*) R. Spitzer, Phys. Rev., 110 (1958) 1190.
G. G. Bach, Nuovo Cimento XI (1959) 73.
R. H. Dalitz, 9th Int. Ann. Conf. on High-Energy Physics, Academy of Sciences, USSR, Vol I (1960) 587.

Microscopic approach to hyperonic matter EOS

input

2BF: nucleon-nucleon (NN), nucleon-hyperon (NY), hyperon-hyperon (YY)
3BF: NNN, NNY, NYY, YYY, 4BF: …….

Phenomenological meson-exchange models:

(Jülich, Nijmegen)

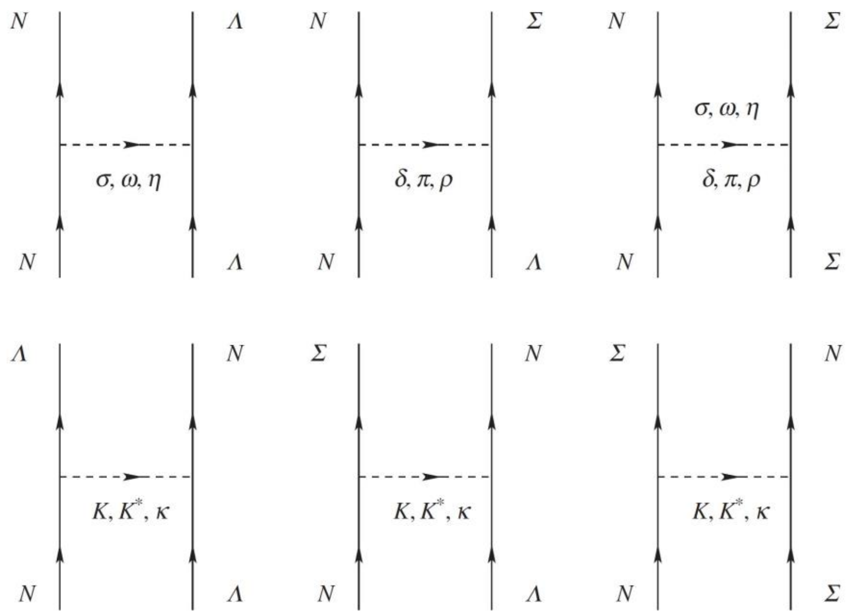

Chiral Effective Field Theory (ChEFT)

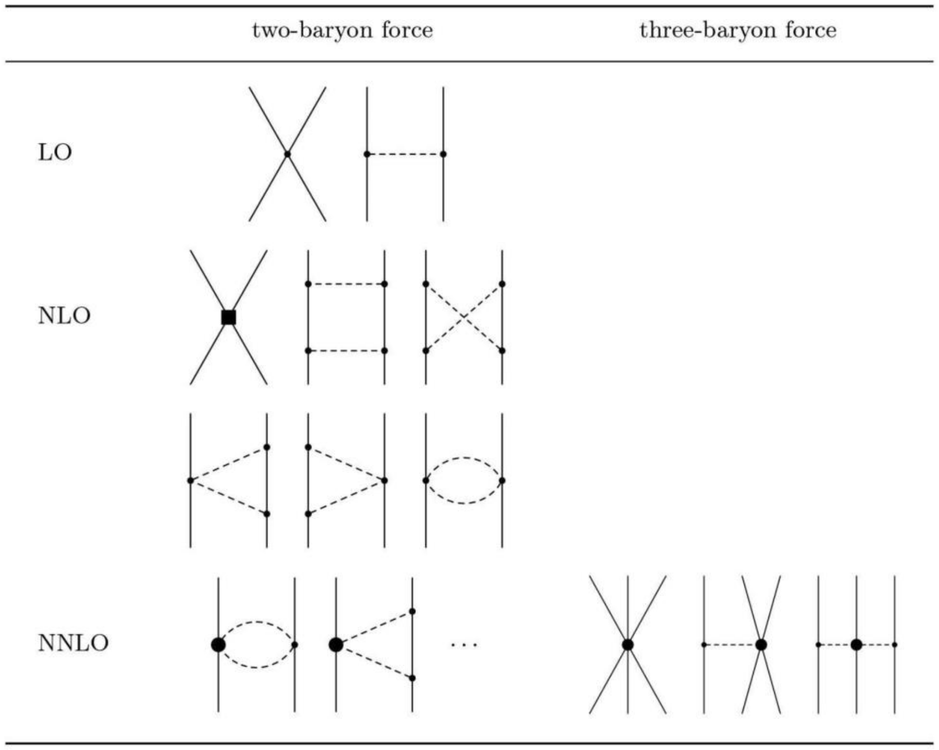

Microscopic approach to hyperonic matter EOS

input

2BF: nucleon-nucleon (NN), nucleon-hyperon (NY), hyperon-hyperon (YY)
3BF: NNN, NNY, NYY, YYY, **4BF:** …….

Hyperonic sector: experimental data

1. YN scattering data ≈ 50
   (NN data ≈ 4300)
2. Hypernuclei : ≈ 40 $_{\Lambda}X$, ≈ 5 $_{\Lambda\Lambda}X$
   a few Ξ^-–hypernuclei
   (nuclei ≈ 3300)

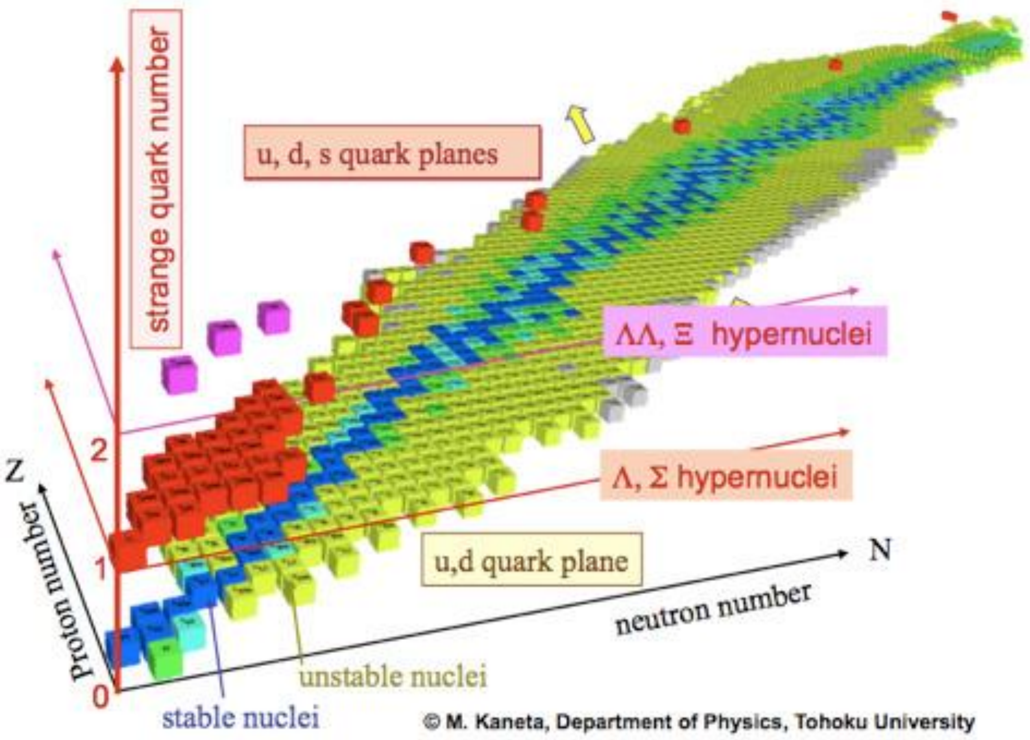

E. Botta, T. Bressani, G. Garbarino, Eur. Phys. J. A 48 (2012) 41
C. Curceanu, *et al.*, Rev. Mod. Phys. 91 (2019) 025006
O. Hashimoto, H. Tamura, Prog. Part. Nucl. Phys. 57, (2006) 564.
L. Tolos, and L. Fabbietti, Prog. Part. Nucl. Phys. 112 (2020) 103770

Hypertriton lifetime and binding energy

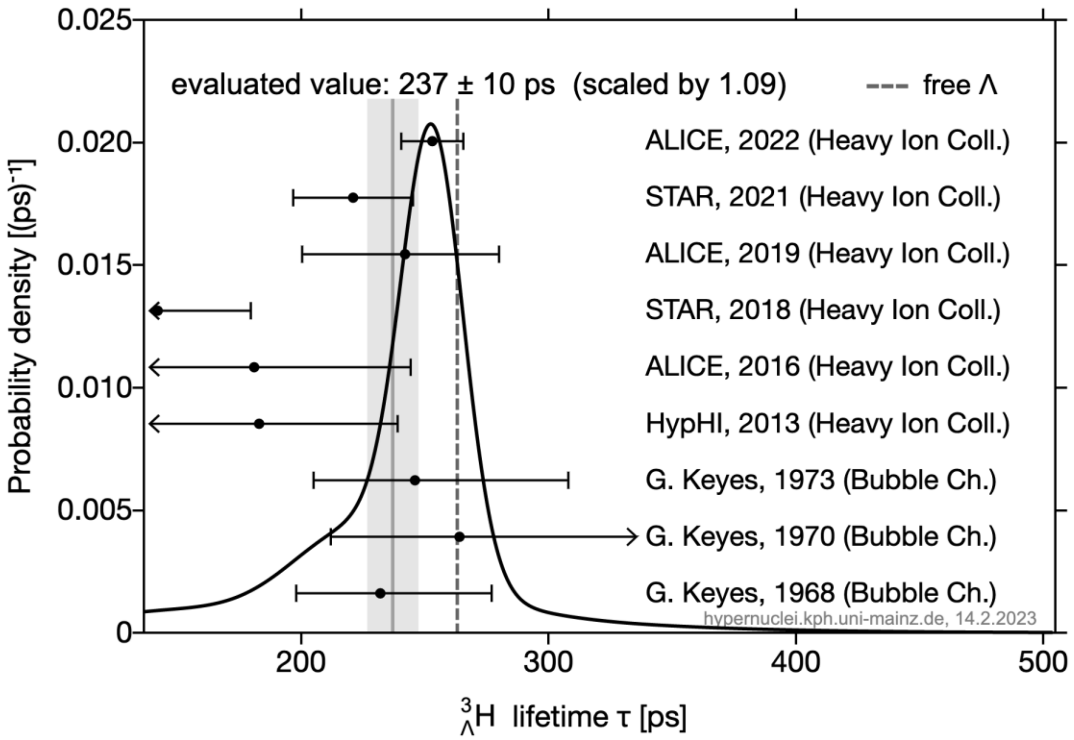

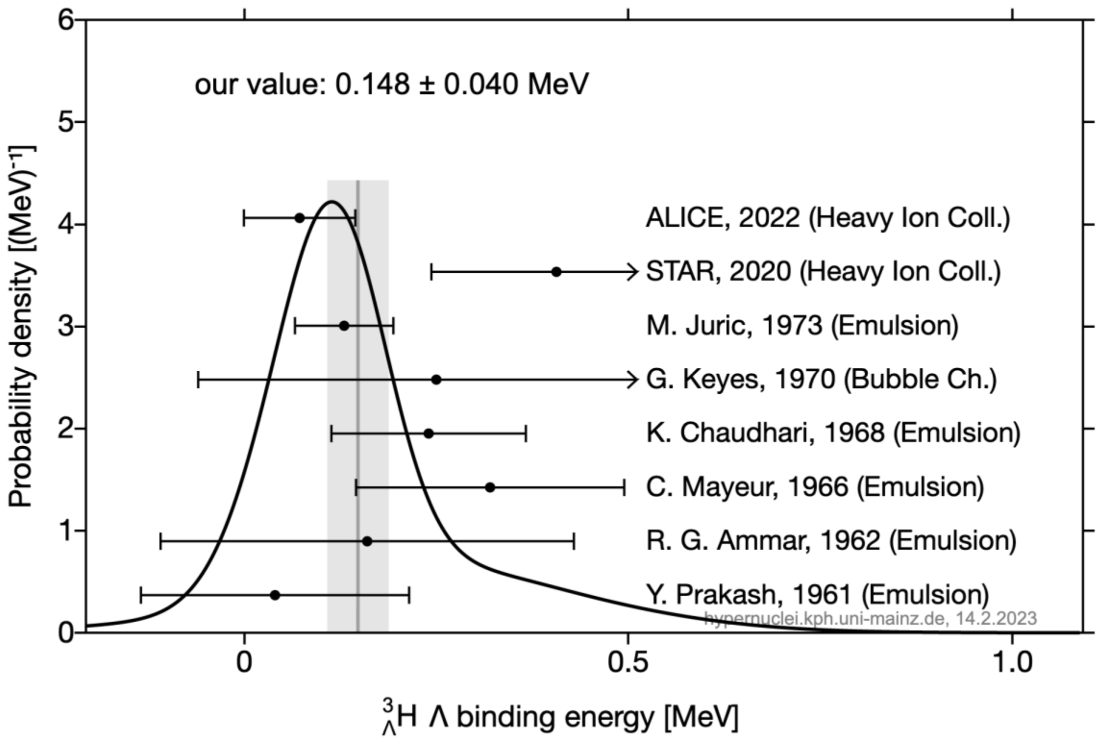

M. Puccio, Day 2 Wrap-Up

A breakthrough for determining the NY and YY interactions

Recently, the **ALICE Collaboration** has demonstrated that **NY** and **YY interactions** can be investigated with high precision using ***p*–*p* and *p*–Pb collisions at the LHC** (using the technique called **femtoscopy**).

ALICE Collaboration. *p*–*p*, *p*–*Λ* and *Λ*–*Λ* correlations studied via femtoscopy in *pp* reactions at $\sqrt{s}$ = 7 TeV. *Phys. Rev. C* 99, 024001 (2019).

ALICE Collaboration. Scattering studies with low-energy kaon–proton femtoscopy in proton–proton collisions at the LHC. *Phys. Rev. Lett*. 124, 092301 (2020).

ALICE Collaboration. Study of the *Λ*–*Λ* interaction with femtoscopy correlations in *pp* and *p*–Pb collisions at the LHC. *Phys. Lett. B* 797, 134822 (2019).

ALICE Collaboration. First observation of an attractive interaction between a proton and a cascade baryon. *Phys. Rev. Lett*. 123, 112002 (2019).

ALICE Collaboration. Investigation of the p–Σ^0 interaction via femtoscopy in *pp* collisions. *Phys. Lett. B* 805, 135419 (2020).

ALICE Collaboration. Unveiling the strong interaction among hadrons at the LHC, Nature 588, 232(2020)

Microscopic EOS for hyperonic matter: extended Brueckner theory

$$G(\omega)_{B_1B_2\,B_3B_4} = V_{B_1B_2\,B_3B_4} + \sum_{B_5B_6} V_{B_1B_2\,B_5B_6} \frac{Q_{B_5B_6}}{\omega - e_{B_5} - e_{B_6}} G(\omega)_{B_5B_6B_3B_4}$$

$$e_{B_i}(k) = M_{B_i}c^2 + \frac{\hbar^2 k^2}{2M_{B_i}} + U_{B_i}(k)$$

$$U_{B_i}(k) = \sum_{B_j} \sum_{k' \le k_{F\,B_j}} \langle \vec{k}\vec{k}' | \, G_{B_iB_j\,B_i\,B_j}(\omega = e_{B_i} + e_{B_j}) \, | \vec{k}\vec{k}' \rangle$$

V is the **baryon -baryon interaction for the baryon octet: n, p, Λ, Σ^-, Σ^0, Σ^+, Ξ^-, Ξ^0**

- **Energy per baryon in the BHF approximation**

$$E/N_B = 2\sum_{B_i}\int_0^{k_F[B_i]} \frac{d^3k}{(2\pi)^3} \left\{ M_{B_i}c^2 + \frac{\hbar^2k^2}{2M_{B_i}} + \frac{1}{2}U^N_{B_i}(k) + \frac{1}{2}U^Y_{B_i}(k) \right\}$$

M. Baldo, G.F. Burgio, H.-J. Schulze, Phys.Rev. C61 (2000) 055801
I. Vidaña, A. Polls, A. Ramos, Engvik, M. Hjorth-Jensen, Phys.Rev. C62 (2000) 035801
I. Vidana, Ph. D. Thesis, Barcelona University (2001)
I. Vidaña, I. Bombaci, A. Polls, A. Ramos, Astron. Astrophys. 399, (2003) 687.

A simplified version for hyperonic matter: {n, p, Λ}-matter

(D. Logoteta, I. Vidaña, I. Bombaci, Eur. Phys. J. A 55 (2019) 207)

Interactions:

NN ChEFT N3LO Δ(1232) Piarulli et al., Phys. Rev. C 94 (2016) 054007

NNN ChEFT N2LO Δ(1232) Epelbaum et al., Phys. Rev C 66 (2002) 064001
Navratil, Few-Body Syst. 41 (2007) 117

average → $V^{eff}_{NN}(n)$ Logoteta et al., Phys. Rev. C 94 (2016) 064001

NΛ Nijmegen Soft Core 97 (NSC97a,e) Rijken et al., Phys. Rev. C 59, (1999) 21;
Stocks , Rijken, Phys. Rev. C 59 (1999) 3009

NNΛ ChEFT N2LO Petschauer et al., Phys. Rev. C 93 (2016) 014001

average → $V^{eff}_{N\Lambda}(n)$ Petschauer et al., Nucl. Phys. A 957 (2017) 347

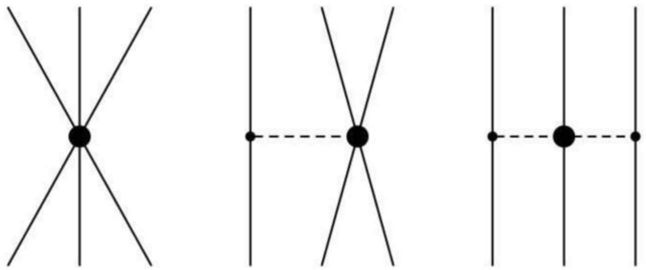

Saturation by decuplet baryons →

Only one **LEC (H')** is left

$$H' = \frac{\beta}{f_\pi^2}$$

$f_\pi = 93$ MeV pion decay constant

We fix **β** to to have, in **symmetric nuclear matter** at the empirical saturation density $\mathbf{n_0 = 0.16\ fm^{-3}}$ **:**

$$U_\Lambda(k=0, n_0) = B_\Lambda^\infty$$

where B_Λ^∞ is the extrapolation to infinite nuclear matter of the **binding energy** $\mathbf{B_\Lambda}$ of **Λ in hypernuclei**

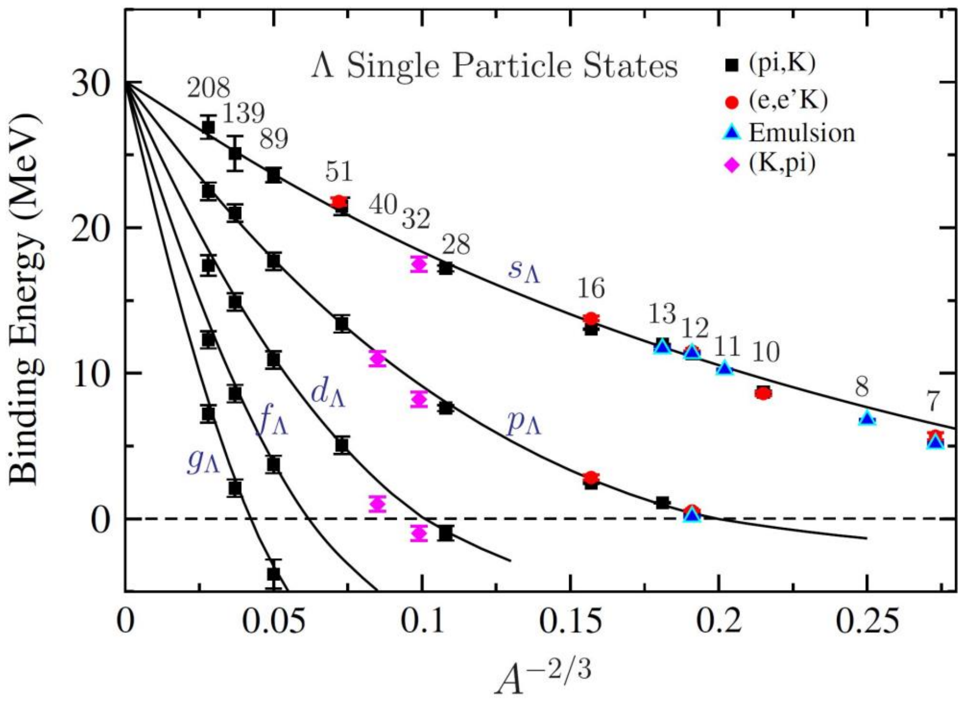

$$U_\Lambda(k=0, n_0) = -28\ \text{MeV} \qquad (\text{NN}\Lambda_1)$$

$$U_\Lambda(k=0, n_0) = -30\ \text{MeV} \qquad (\text{NN}\Lambda_2)$$

D. Logoteta, I. Vidaña, I. Bombaci, Eur. Phys. J. A 55 (2019) 207

Hyperonic three-body interactions could represent a likely solution of the hyperon puzzle in Neutron Stars

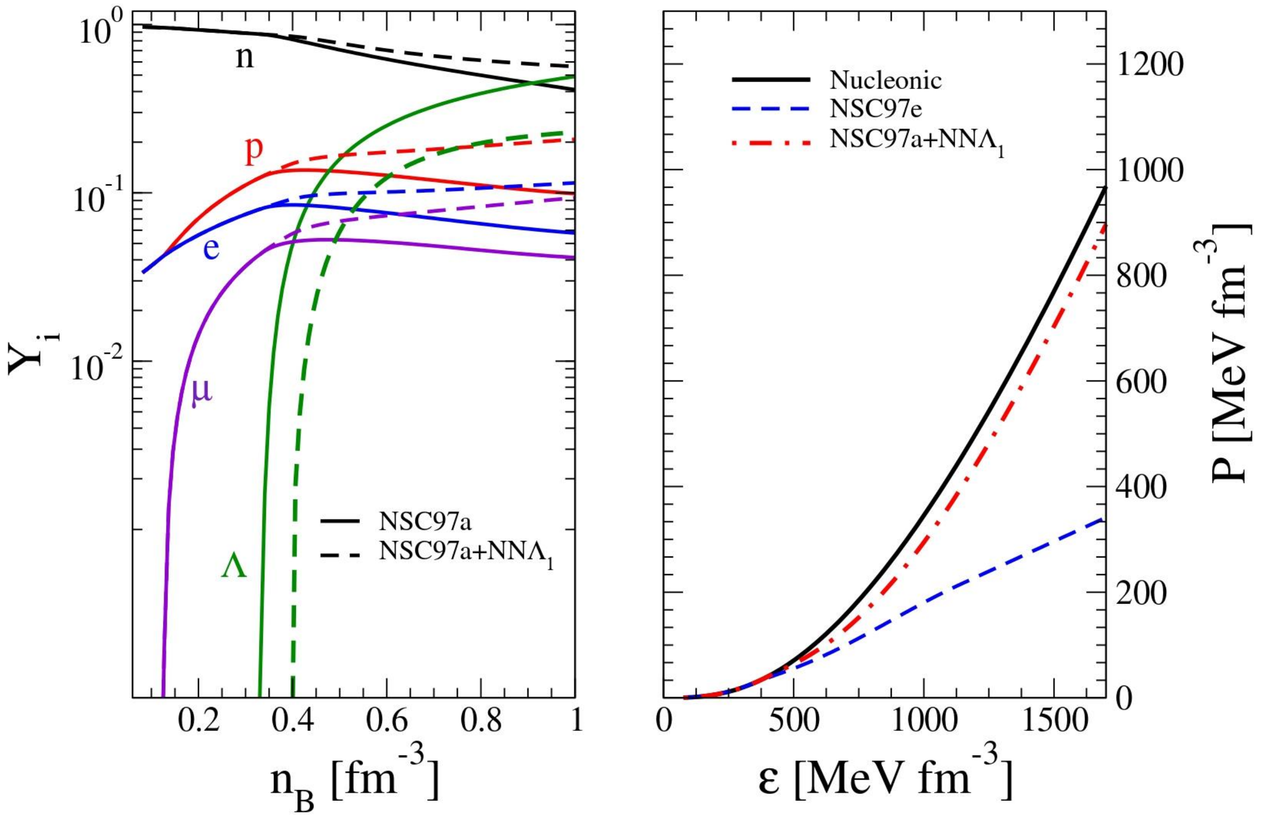

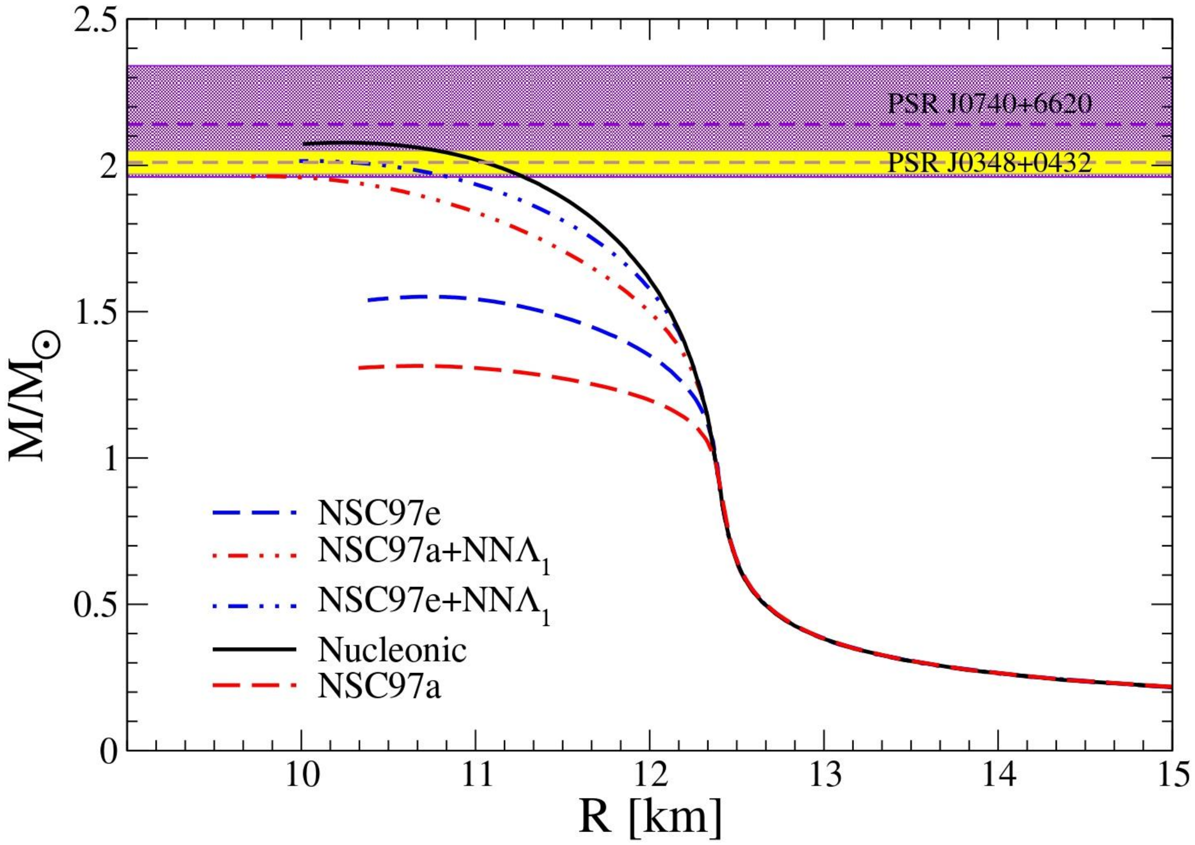

D. Logoteta, I. Vidaña, I. Bombaci, Eur. Phys. J. A 55 (2019) 207

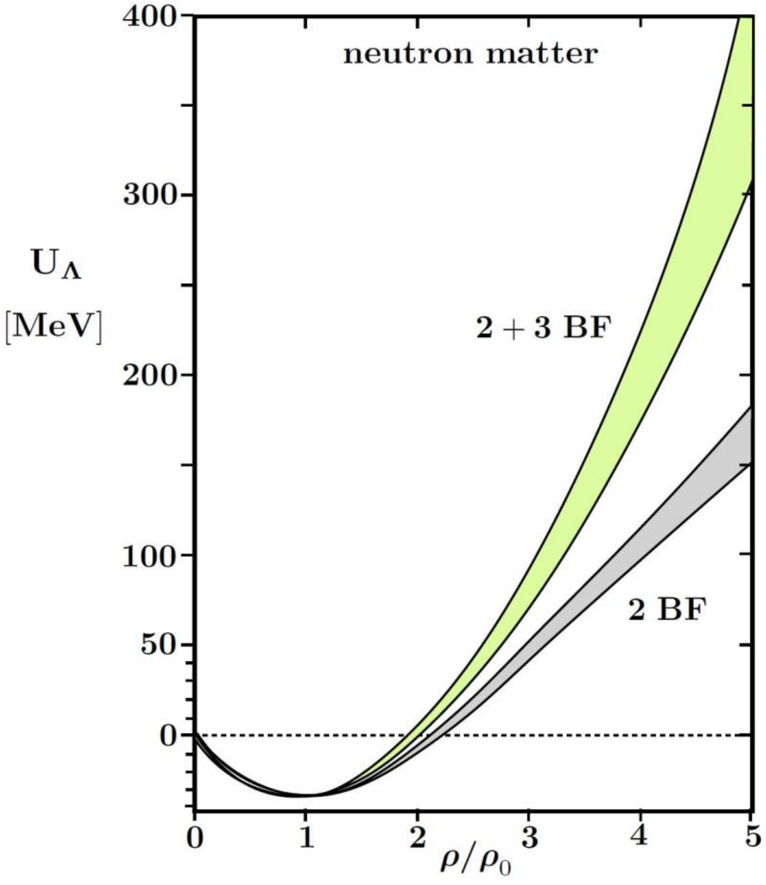

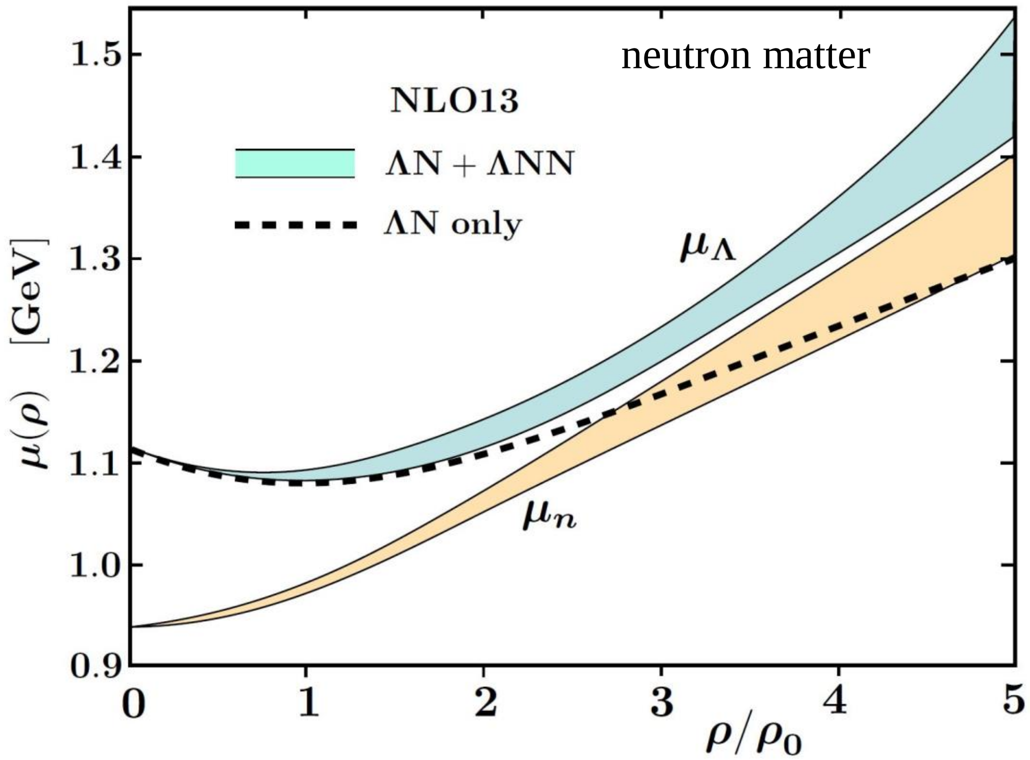

D. Gerstung, N. Kaiser, W. Weise, Eur. Phys. J. A 56 (2020) 175

«The combined repulsion from two- and three-body hyperon-nuclear interactions can indeed be potentially strong enough to avoid the appearanche of Λ hyperons in neutron stars»

The hyperon puzzle in Neutron Stars

Hyperonic three-body interactions could represent a likely solution of the hyperon puzzle in Neutron Stars

but

if hyperonic three-body interactions are repulsive enough, hyperons will never appear at the densities encountered in neutron star cores.

In this case "hyperon stars" would not contain hyperons at all, that is, we will go back to the case of **nucleonic stars**.

This could be a physically acceptable conclusion if the "true" hyperonic three-body interactions make **hyperon formation non convenient from an energetic point of view**, **contrary to the simple expectation based on** **ideal Fermi gas argument.**

Quark Matter in Neutron Stars and in BNS mergers

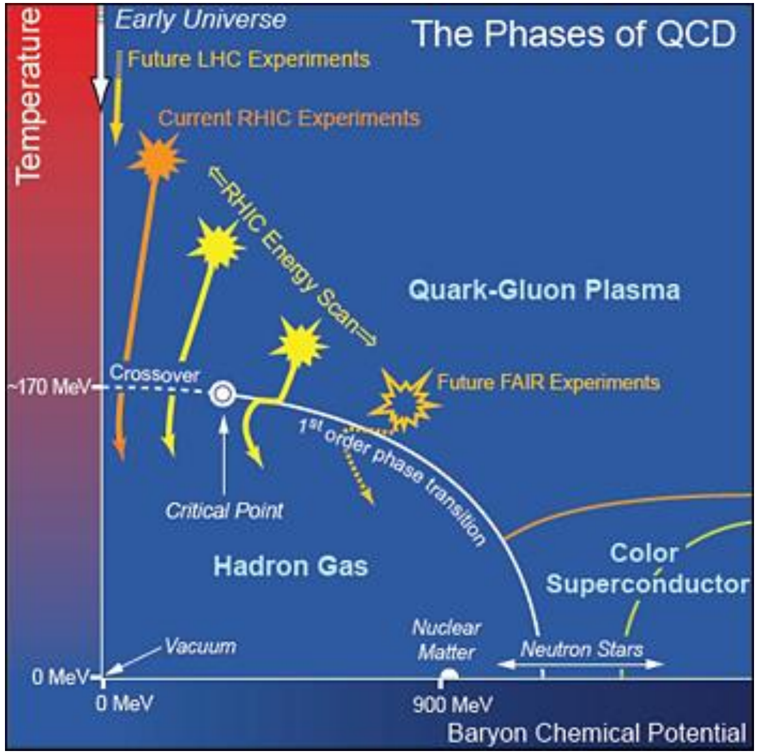

Can GW observations test the possible occurence of a quark-deconfinement phase transtion in NS matter ?

The Dynamics of Binary Neutron Star Mergers

1) Early-inspiral phase

point-like objects, $d >> d_{merg} \equiv \min\left[(R_1 + R_2),\ \frac{6G}{c^2}(M_1 + M_2) \right]$

No EoS dependence (except M_{max}(EoS))

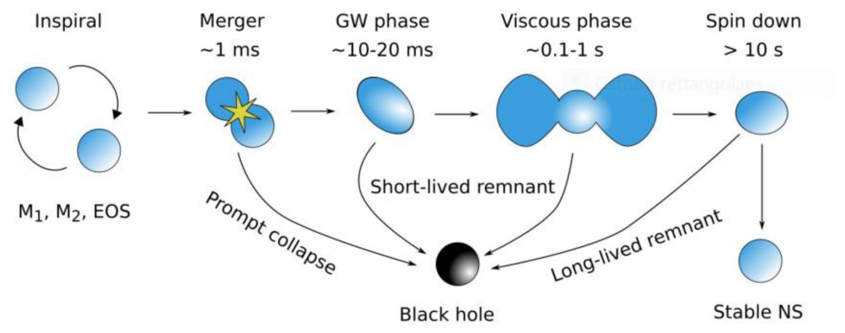

2) Inspiral phase

$d \approx (1 \div 10)\ d_{merg}$

tidal deformations of NSs $Q_{ij} = \lambda\ \varepsilon_{ij}$

EoS : cold (T = 0) , neutrino-free matter

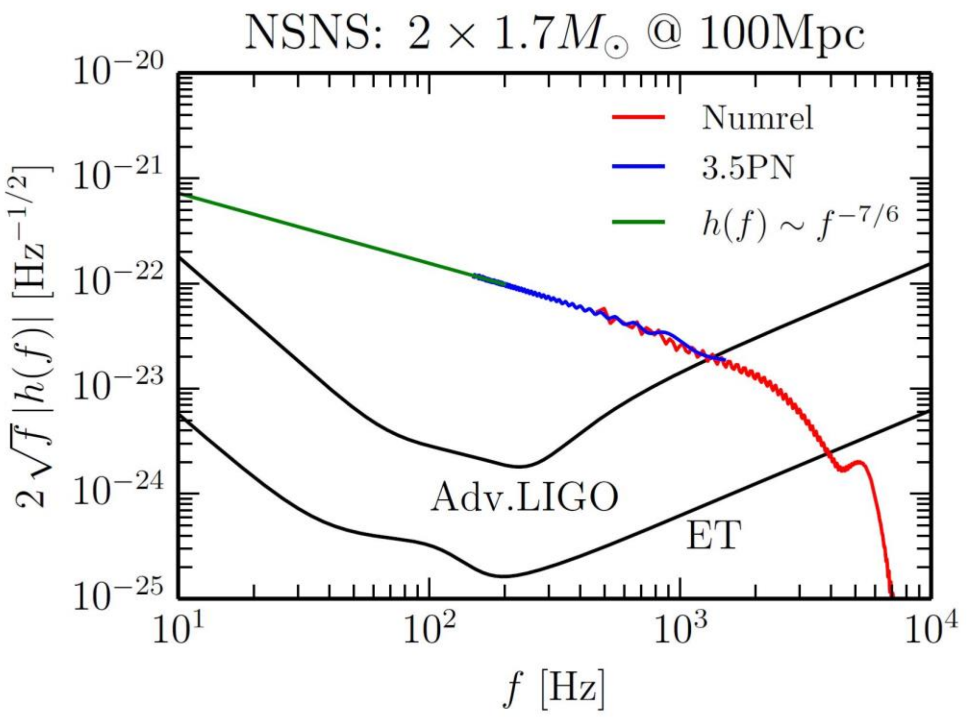

3) Merger, post-merger compact object

rapidly-differentially-rotating proto-NS

EoS : hot (T = 10–100 MeV) , neutrino-trapped matter

$t_{weak} \sim 10^{-9}$ s , $t_{trapp} \sim (10 - 30)$ s

4) Post-merger evolution: final merger remnant

- **prompt Black Hole formation**
- **hyper-massive proto-NS** → **delayed BH formation**
  - differ .→ rigid rot.
- **metastable proto-NS** (ν-escape & cooling)
  - → **delayed BH formaion**
  - → **stable fast-rotating NS**

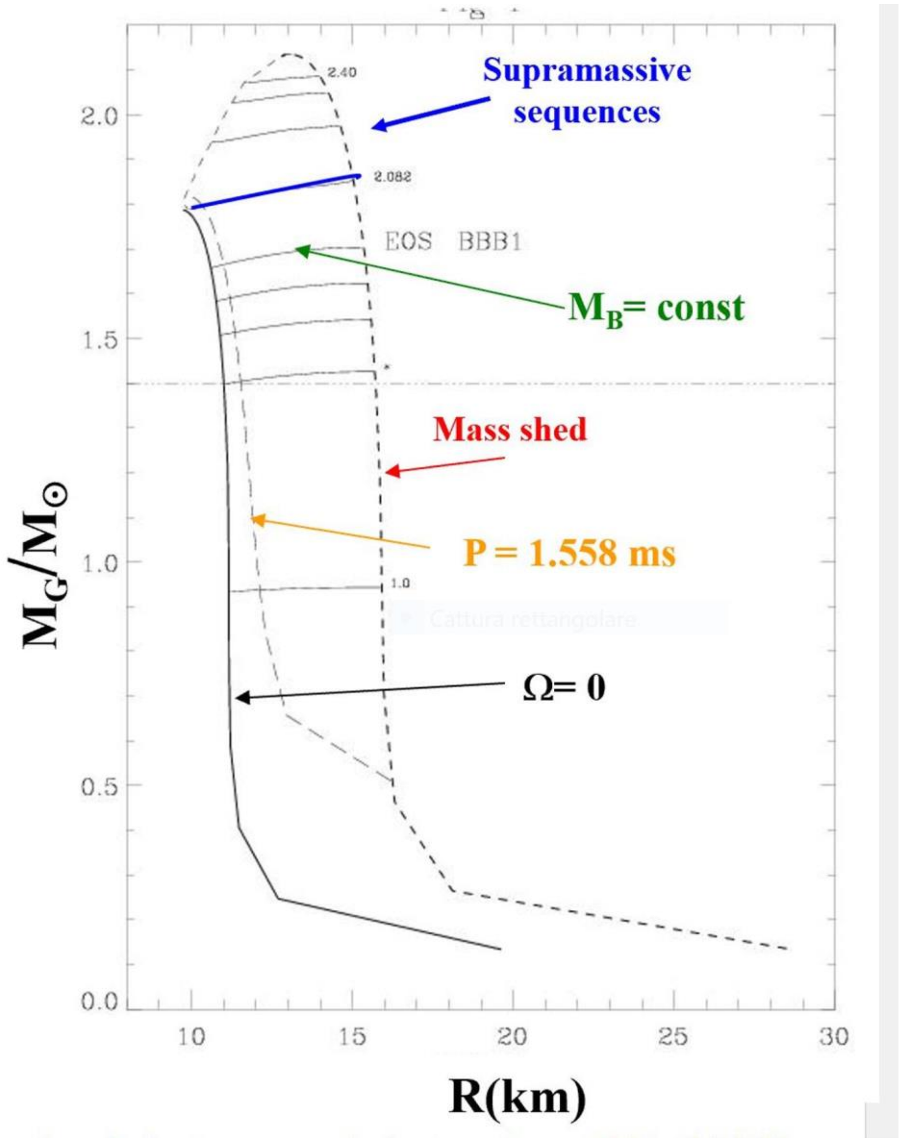

B. Datta, A.V. Thampan, I. Bombaci, A&A 334 (1998)

Modeling extreme matter and GWs with piecewise-polytropic EOS

$$P(\rho) = K_i \, \rho^{\Gamma_i} \, ; \quad \varrho_{i-1} \leq \rho \leq \varrho_i$$

Advantages:
very easy and efficient to use in GR numerical simulations;
Easy to include physical requirements as e.g. causality condition,
and $M_{max} \geq 2 \, M_\odot$

Disadvantages:
No informations on the particle composition of matter.
No connection with the underlying microphysics of the strong interactions.
No fundamental physics of dense matter modeling BNS mergers with polytropic EOS

G. Raaijmakers, T.E. Riela, A.L. Watts,
A pitfall of piecewise-polytropic equation of state inference, MNRAS 478 (2018) 2177

EOS for SQM: extended bag model (at finite temperature)

$$\Omega = \sum_{i=u,d,s} \Omega_i^0 + \frac{3}{4\pi^2}(1-a_4)\left(\frac{\mu_b}{3}\right)^4 + B_{eff}$$

$$\varepsilon = \sum_{i=u,d,s} \Omega_i^0 + \frac{3}{4\pi^2}(1-a_4)\left(\frac{\mu_b}{3}\right)^4 + \sum_{i=u,d,s} \mu_i n_i + B_{eff}$$

$\hbar = 1 \quad c = 1$

2nd term = perturbative QCD correction up to $O(\alpha_s^2)$

$a_4 = 1$ (ideal relativistic gas + bag constant)

$$\mu_b = \mu_u + \mu_d + \mu_s$$

$$n_b = \frac{1}{3}(n_u + n_d + n_s)$$

$$\mu_s = \mu_d = \mu_u + \mu_e$$

$$\frac{2}{3}n_u - \frac{1}{3}n_d - \frac{1}{3}n_s - n_e = 0$$

E. Fraga, R.D. Pisarki, J. Schaffner-Bielich, Phys. Rev. D 63 (2001) 12172(R)
M. Alford, M. Braby, M. Paris, S. Reddy, ApJ 629 (2005) 969
S. Weissenborn, I. Sagert, G. Pagliara, M. Hempel, J. Schaffner-Bielich, ApJ 740 (2011) L14

Isoentropic β-stable hybrid matter

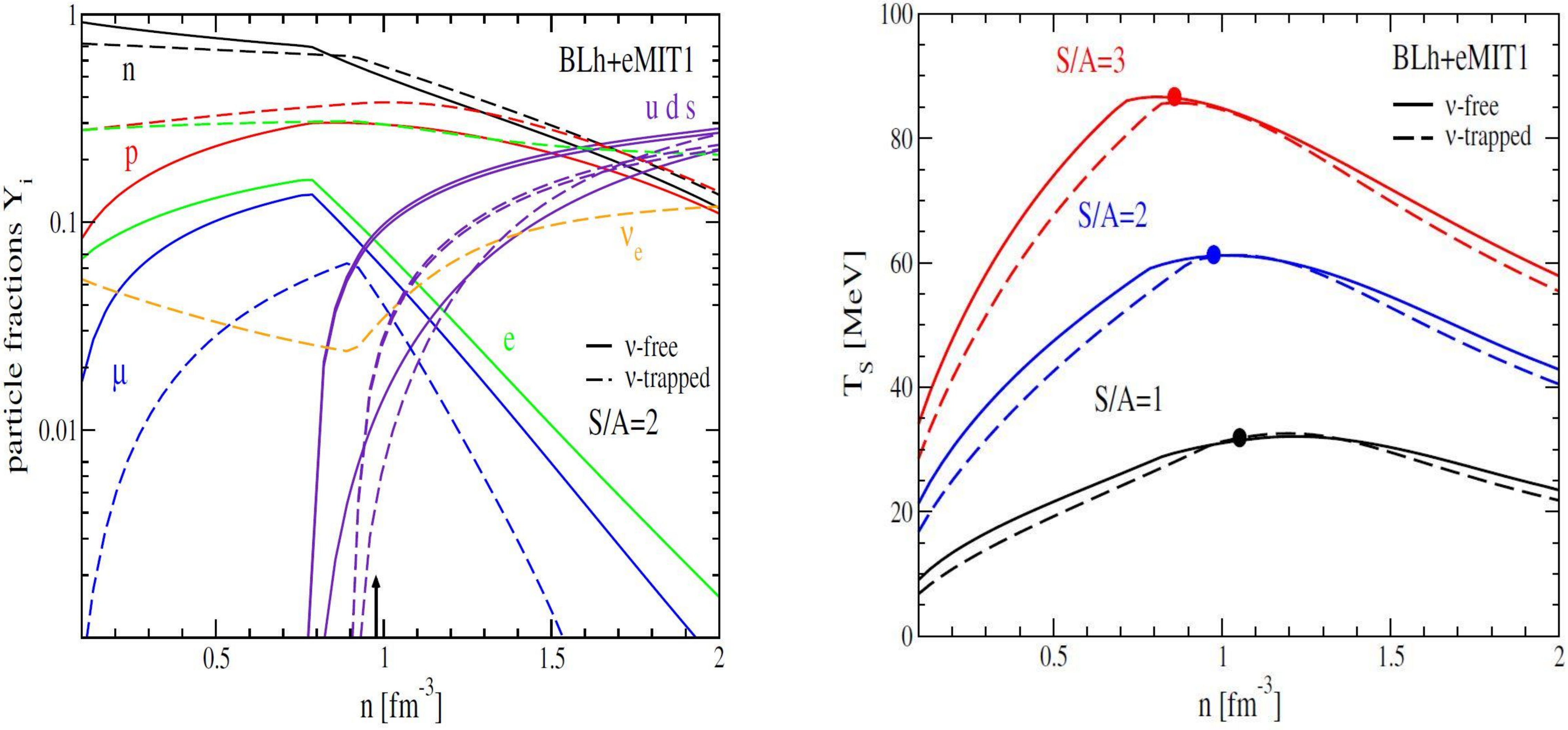

D. Logoteta, I. Bombaci, A. Perego, Eur. Phys. J. A 58 (2022)

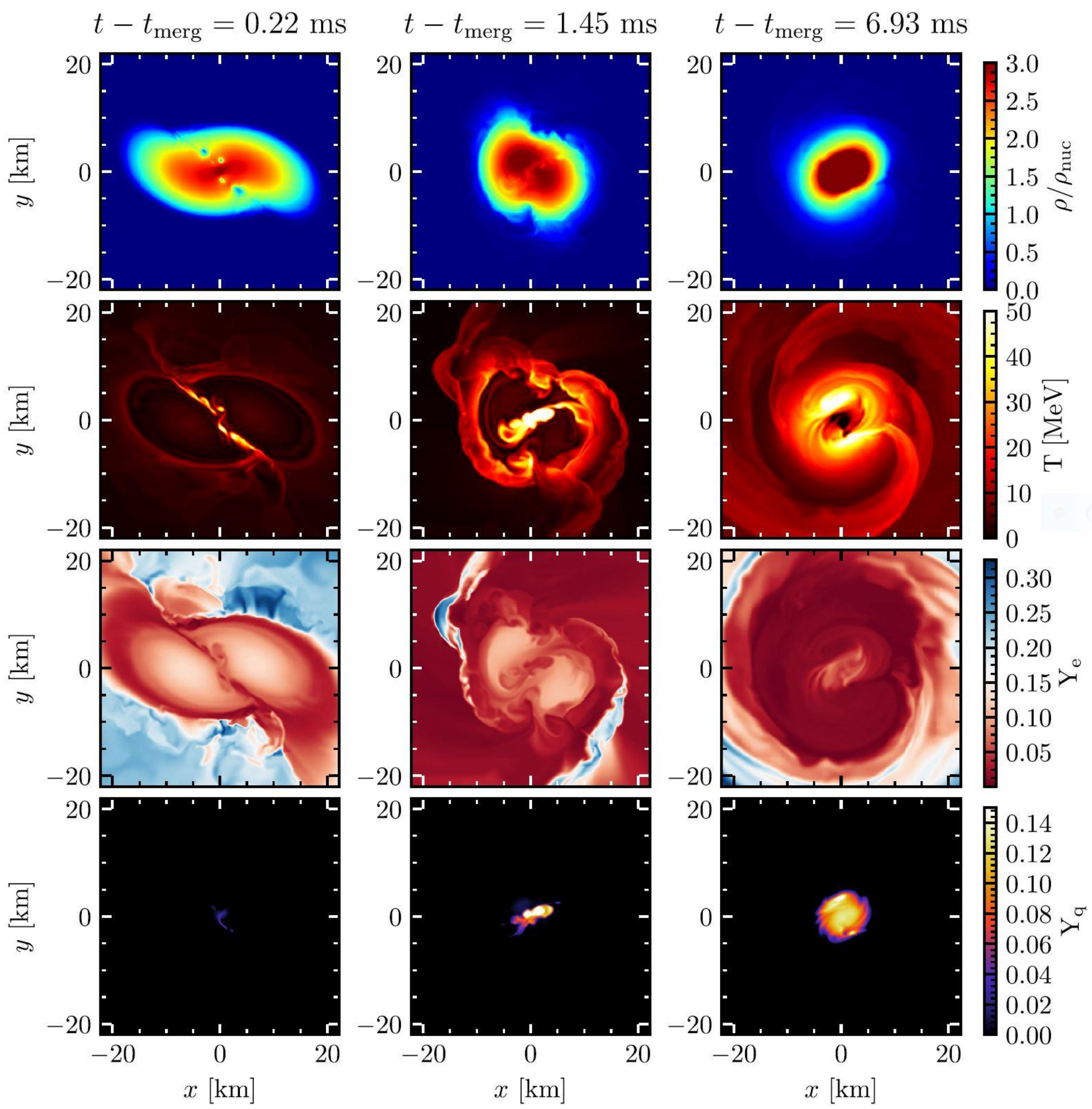

BNS mergers numerical simulations

Full General Relativistic Hydrodynamics

Code: Wisky THC

D. Radice, L. Rezzolla, Astron. & Astrophys. 547 (2012)

EOS:

BLh finite temperature nuclear matter (BHF)

BLQ finite temperature EOS for hybrid nuclear-quark matter

A. Prakash, D. Radice, D. Logoteta, A. Perego, V. Nedora, I. Bombaci, R. Kashyap, S. Bernuzzi, A. Endrizzi, Phys. Rev. D104 (2021)

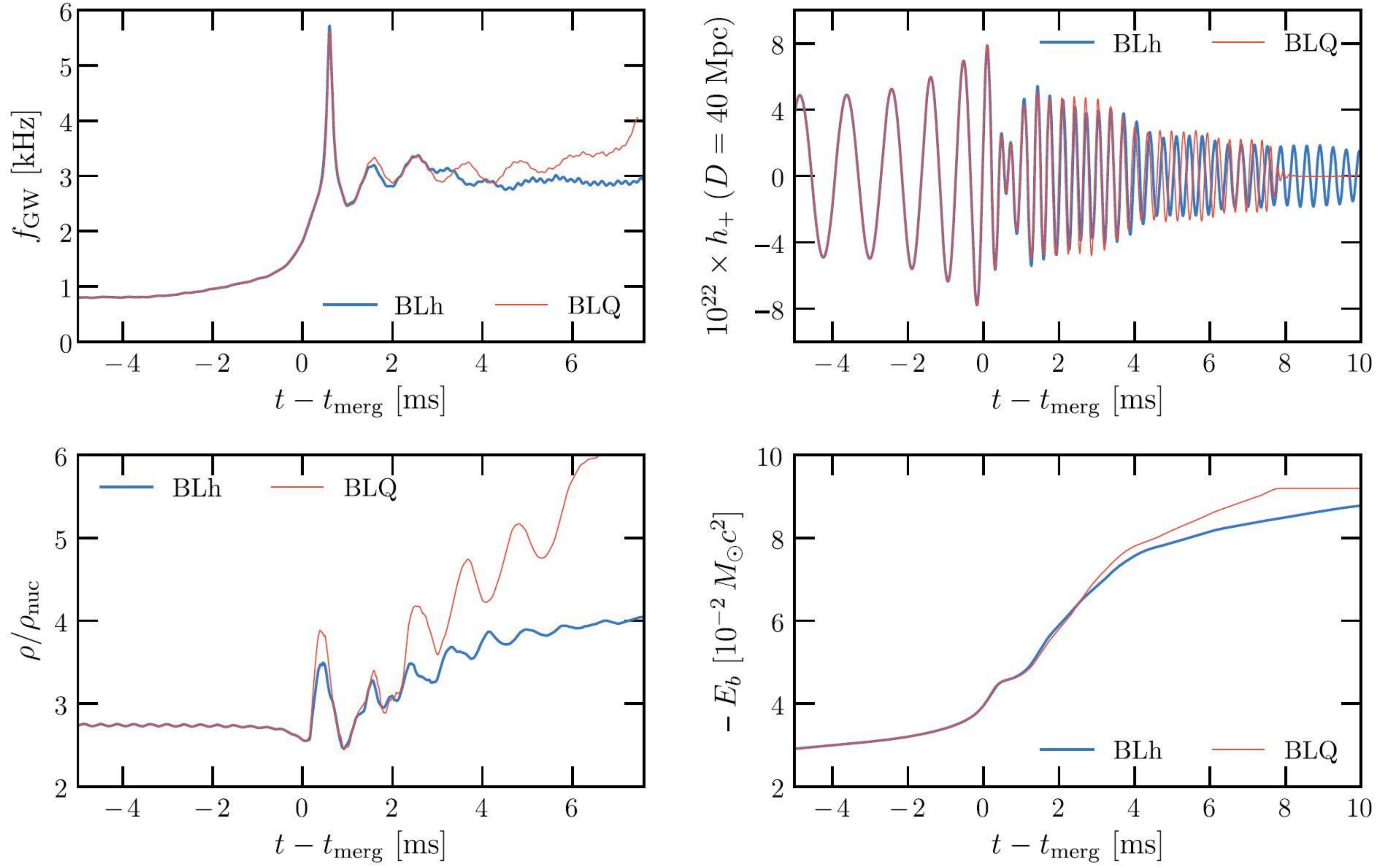

FIG. 7. Evolution of the instantaneous GW frequency $f_{\rm GW}$, the "+" polarization strain amplitude for the $(l = 2, m = 2)$ mode of the GW signal, the central density ρ, and the binding energy E_b of the 1.3325–1.3325 $M_\odot$ binary. The inspiral $(t \leq t_{\rm merg})$ evolution predicted by both the BLh and BLQ EOSs is identical. The appearance of quarks is imprinted on the postmerger dynamics and GW signal.

A. Prakash, D. Radice, D. Logoteta, A. Perego, V. Nedora, I. Bombaci, R. Kashyap, S. Bernuzzi, A. Endrizzi, Phys. Rev. D104 (2021)

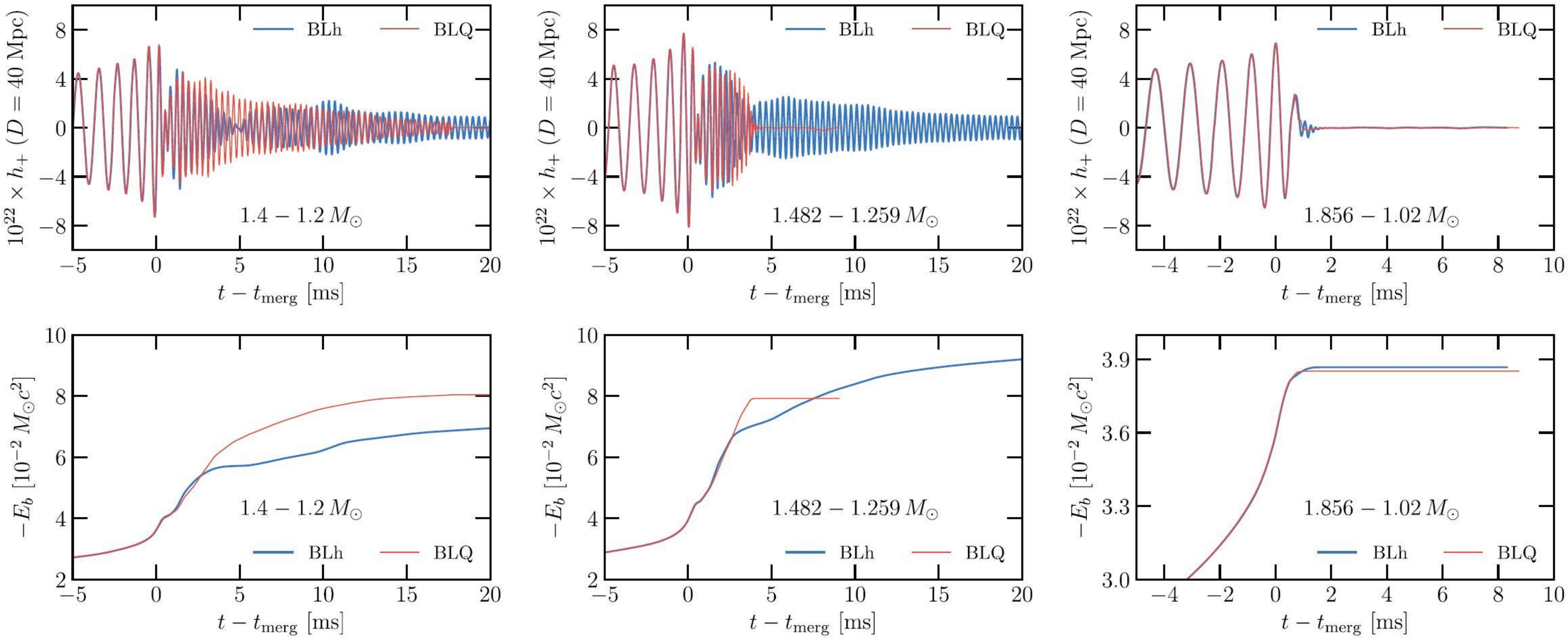

FIG. 8. Amplitude of the ($l = 2$, $m = 2$) mode of the GW strain h_+ and binding energies for the 1.4–1.2 $M_\odot$, 1.482–1.259 $M_\odot$, and 1.856–1.020 $M_\odot$ binaries. As the binaries become more massive or more asymmetric, the length of the postmerger signal decreases. The postmerger is further shortened by an onset of deconfinement phase transition.

A. Prakash, D. Radice, D. Logoteta, A. Perego, V. Nedora, I. Bombaci, R. Kashyap, S. Bernuzzi, A. Endrizzi, Phys. Rev. D104 (2021)

Identifying a first-order phase transition in NS mergers through GWs

A. Bauswein et al. Phys. Rev. Lett. 122 (2019) 061102

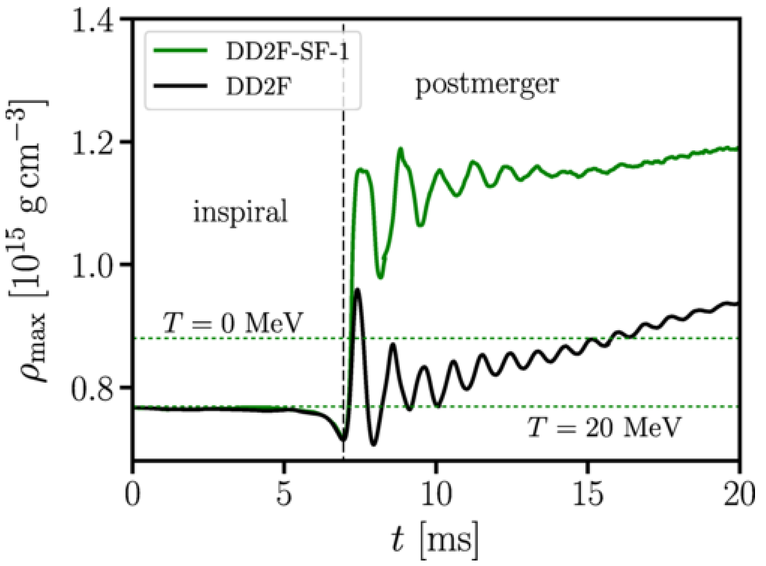

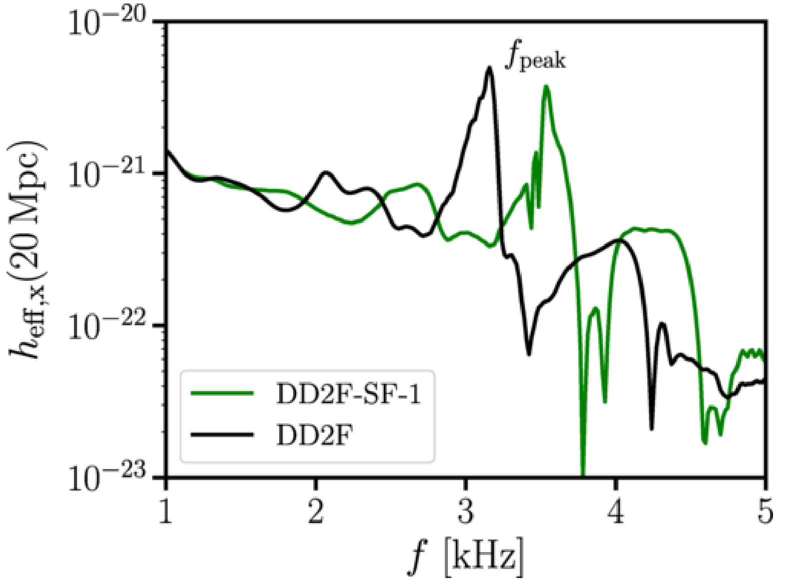

f_{peak} = **frequency of the dominant oscillation of the post-merger object**

This frequency peak is a robust feature that occurs in all the simulaions which do not form directly a black hole **(no prompt BH formation)**

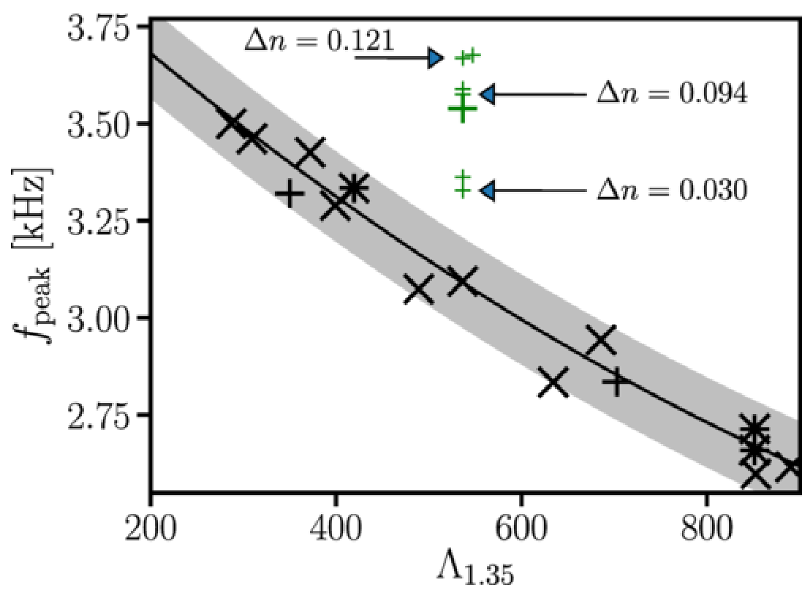

$f_{peak} = f_{peak}(\Lambda)$ **empirical relation**

A significant deviation of the $f_{peak}(\Lambda)$ empirical relation would provide evidence for a **strong first-order phase transition to quark matter.**

This results depends on the **phase-transition construction.**
The authors used the **Maxwell construction**

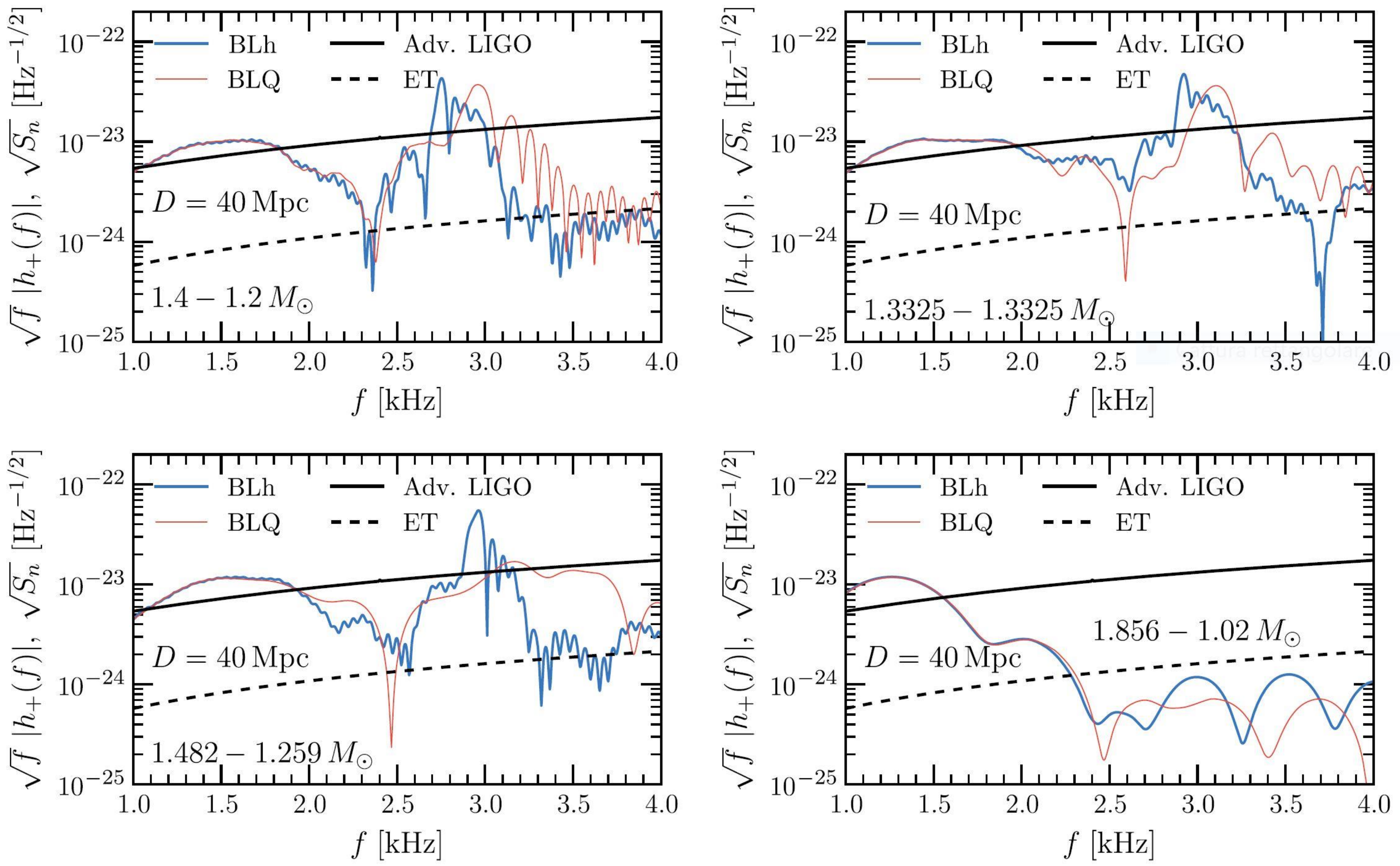

Power spectrum of the (ℓ =2, m = 2) mode of the GW strain

A. Prakash, D. Radice, D. Logoteta, A. Perego, V. Nedora, I. Bombaci, R. Kashyap, S. Bernuzzi, A. Endrizzi, Phys. Rev. D104 (2021)

Probing dense QCD matter in the laboratory

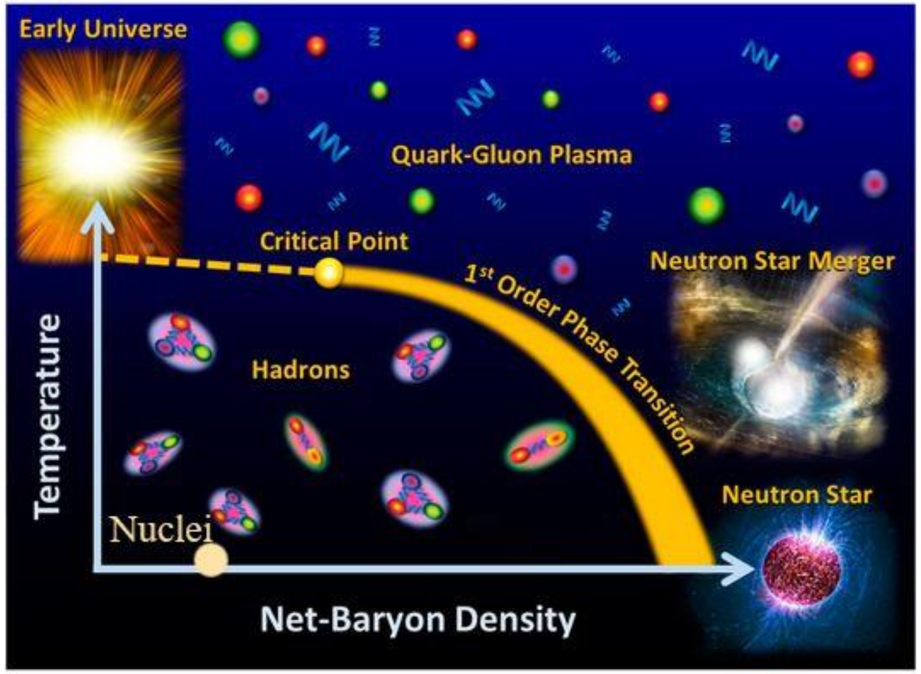

Adapted from P. Senger, and N. Herrmann, Nuclear Physics News, Vol. 28, No 2 (2018) 23.

Whether the **quark-deconfinement phase transition** is of the **first-order with a critical endpoint**, or whether it proceedes smothly by a **crossover** is still an open question.

New dedicated experiments are under construction at future facilities

Compressed Baryonic Matter (CBM) experiment at the Facility for Antiproton and Ion Research (**FAIR**) in **Darmstadt**,

J-PARC Heavy-Ion-project at the Japan Proton Accelerator Research Complex (**J-PARC**) in **Tōkai**,

Heavy-Ion-program at the Nuclotron-based Ion Collider fAcility (**NICA**) at the Joint Institute for Nuclear Research in **Dubna**.

Summary

- The EoS of matter at supranuclear densities is a key ingredient to describe Neutron Stars and related astrophysical phenomena (SNEs, NS-NS merging, GRBs)

- Experimental data of low-energy nuclear physics (NN scattering, properties of atomic nuclei, ….) can constrain the EoS around the empirical saturation point of nuclear matter.

- At supranuclear density various particle species (e.g. hyperons) and phases of matter (e.g. quark deconfined matter) are expected.
  Needs of new experimental data e.g. from hypernuclear physics to constraint models of NY (nucleon-hyperon), YY, NNY, NYY, YYY interactions.
  Relativistic Heavy Ions experiments to explore the QCD phase diagram in the region relevant for NSs, SNe, BNS mergers

- Gravitational wave astronony and multimessanger astrophysics opens a new window to explore the properties of exteme matter


thank you
danke
рахмат
謝謝
ngiyabonga
teşekkür ederim
Баярлалаа
спасибо
mersi
barka
welalin
tack
dank je
gracias
tapadh leat
mahalo
blagodaram
matondo
paldies
хвала
asante
manana
bedankt
dziękuję
hvala
mauruuru
köszönöm
enkosi
mochchakkeram
djiere dieuf
mamnun
chnorakaloutioun
gracies
sulpay
go raibh maith agat
obrigado
sukriya
kop khun krap
taiku
sagolun
dékuji
arigatō
takk
dakujem
trugarez
ありがとう
tanemirt
grazie
mesi
najis tuke
terima kasih
rahmet
diolch
dhanyavadagalu
shukriya
мерси
감사합니다
xiexie
ευχαριστώ
merci

Extra slides

Nuclear interactions derived in Chiral Perturbation Theory (ChPT)

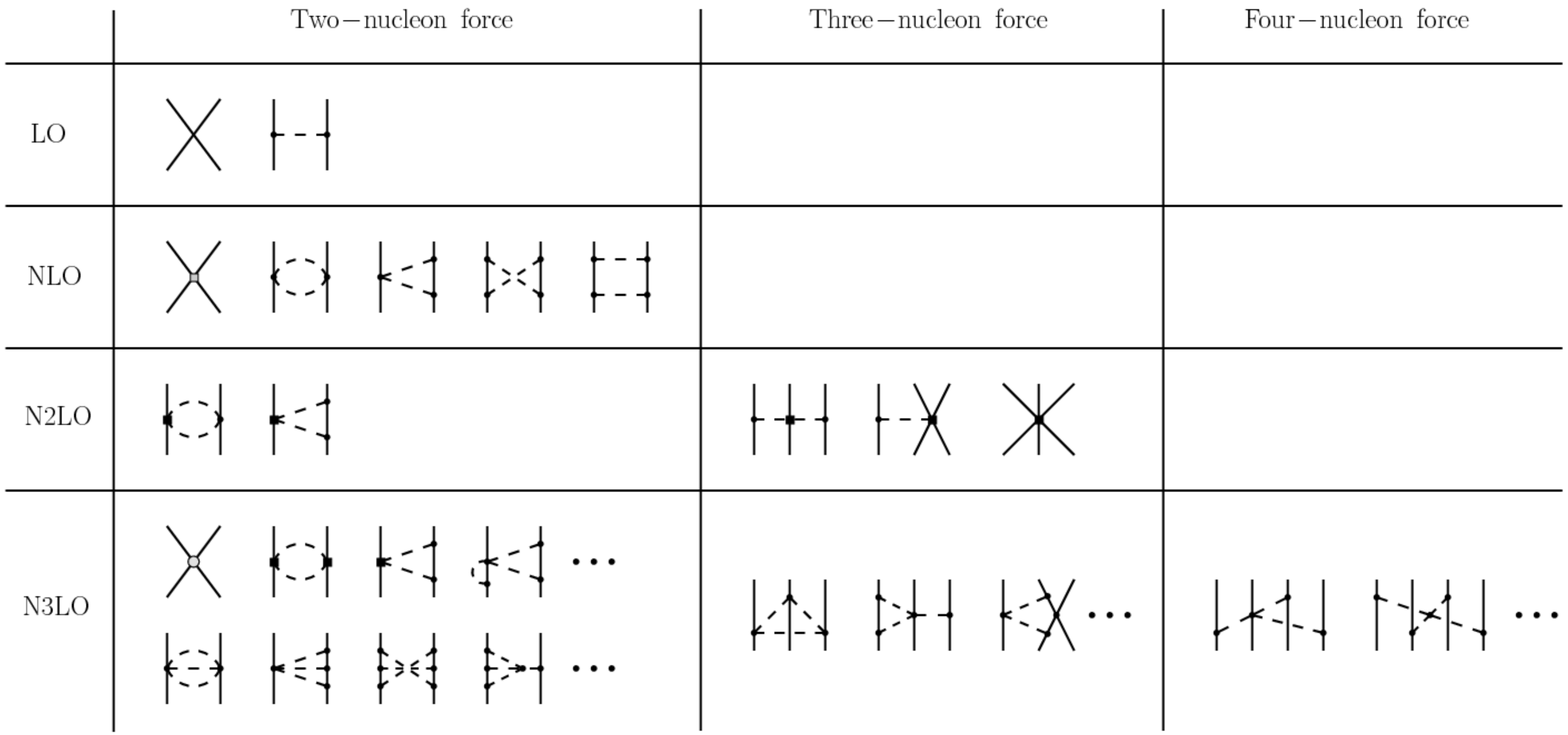

Two-nucleon (NN), three-nucleon (NNN) and many-nucleon intercations can be calculated perturbatively (i.e. order by order) according to a well-defined scheme based on a low-energy effective QCD Lagrangian.

S. Weinberg, Physica A 96 (1979) 327; Phys. Lett. B 251 (1990) 288; Phys. Lett B 259 (1992) 114
E. Epelbaum, H.-W. Hammer, U. G. Meißner, Rev. Mod. Phys. 81 (2009) 1773
R. Machleidt and D. R. Entem, Phys. Rep. 503 (2011) 1
S. Petschauer, J. Haidenbauer, N. Kaiser, , U. G. Meißner, W. Weise, Front. Phys. 8 (2020) 12

Quantum many-body approach

Brueckner-Bethe-Goldstone theory

$$G_{\tau\tau'}(\omega) = V + V \sum_{k_a k_b} \frac{|k_a k_b\rangle Q_{\tau\tau'} \langle k_a k_b|}{\omega - e_\tau(k_a) - e_{\tau'}(k_b) + i\varepsilon} G_{\tau\tau'}(\omega)$$

$$e_\tau(k) = \frac{\hbar^2 k^2}{2m} + U_\tau(k)$$

$$U_\tau(k) = \Re\left\{ \sum_{\tau'} \sum_{k'} \langle kk' | G_{\tau\tau'}(e_\tau(k) + e_{\tau'}(k')) | kk' \rangle_A \right\}$$

Energy per baryon in the Brueckner-Hartree-Fock (BHF) approximation

$$\tilde{E}(n_n, n_p) \equiv \frac{E}{A} = \frac{1}{A}\left\{ \sum_\tau \sum_k \frac{\hbar^2 k^2}{2M} + \frac{1}{2} \sum_\tau \sum_k U_\tau(k) \right\}$$

$$n_n = \frac{1}{2}(1+\beta)n$$

$$n_p = \frac{1}{2}(1-\beta)n$$

Saturation by decuplet baryons

	three-baryon force	
	decuplet-less EFT	decuplet-contribution
LO		
NLO		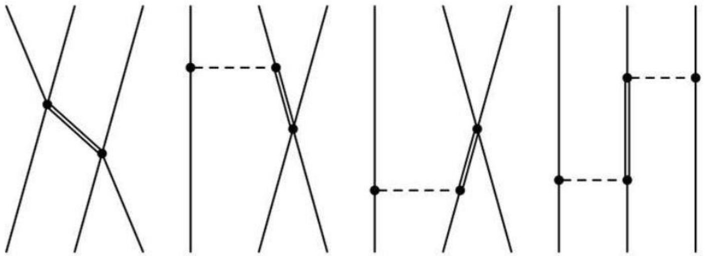
NNLO	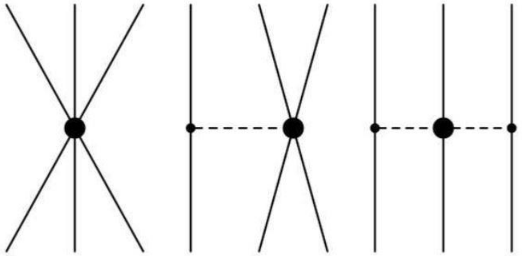	...

Tidal deformability and Love number

$$Q_{ij} = \lambda \quad \varepsilon_{ij}$$

$$\lambda = \frac{2}{3}\frac{k_2}{G}R^5$$

$$\Lambda = \frac{2}{3}k_2\left(\frac{c^2 R}{GM}\right)^5$$

Binary tidal deformability

$$\tilde{\Lambda} = \frac{16}{13}\frac{(m_1+12m_2)\, m_1^4\, \Lambda_1 + (m_2+12m_1)\, m_2^4\, \Lambda_2}{(m_1+m_2)^5}$$

$$\tilde{\Lambda} = \frac{16}{13}\frac{(12q+1)\Lambda_1 + (12+q) \quad q^4\Lambda_2}{(1+q)^5}$$

$$M_{chirp} = \frac{(m_1 m_2)^{3/5}}{(m_1+m_2)^{1/5}}$$

$$M_{chirp} = \left[\frac{q}{(1+q)^2}\right]^{3/5} M_{tot}$$

$$q = \frac{m_2}{m_1} \leq 1$$

T. Hinderer, ApJ 677 (2008) 1216; erratum arXiv:0711.2420

T. Damour and A. Nagar, Phys. Rev. D 80 (2009) 084035

T. Damour, A. Nagar and L. Villain, Phys. Rev. D 85 (2012) 123007

S. Postikov, M. Prakash ans J. M. Lattimer, Phys. Rev. D 82 (2010)

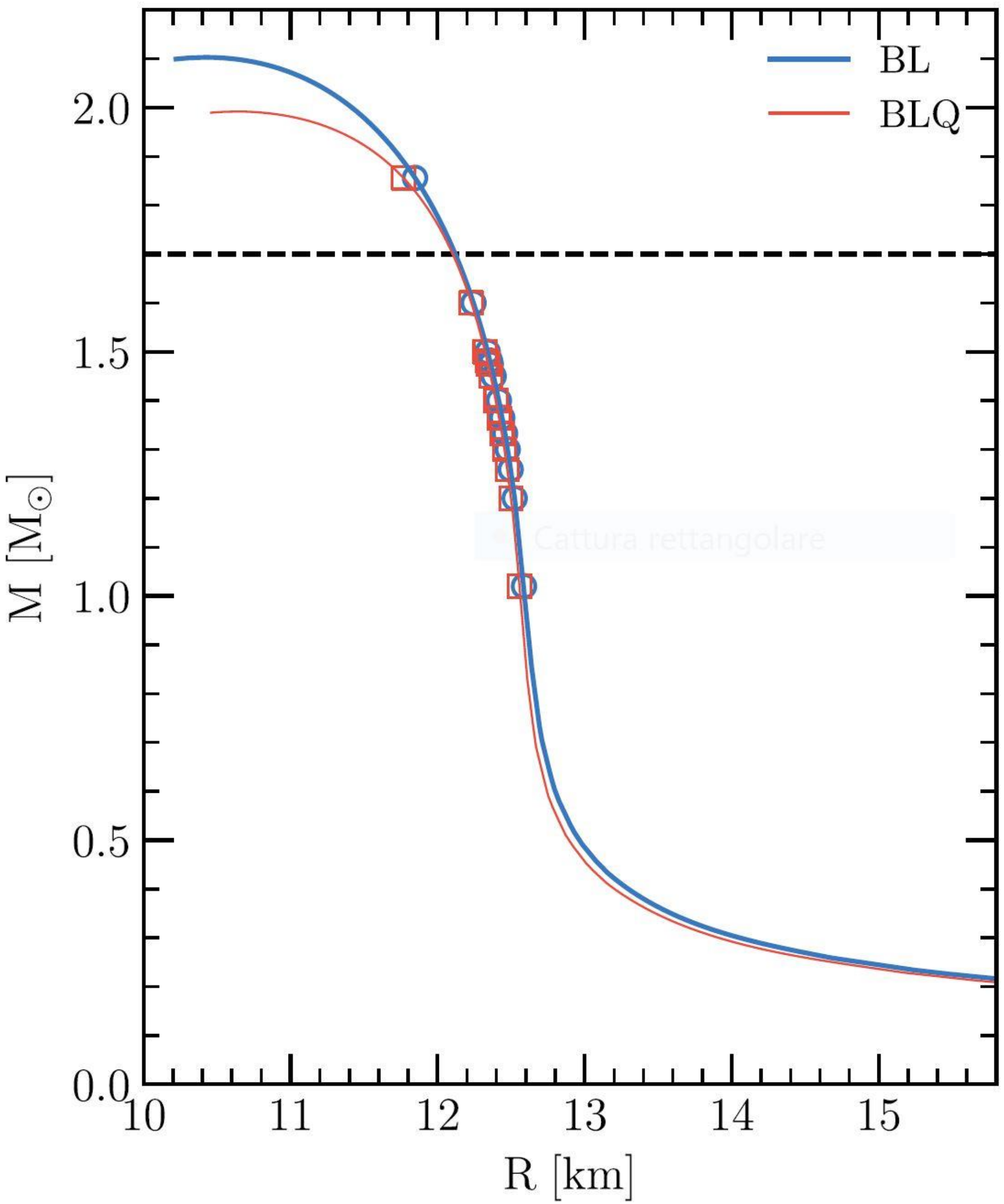

BL
BLQ
M [M$_\odot$]
R [km]
0.0
0.5
1.0
1.5
2.0
10
11
12
13
14
15

First-order phase transitions: phase equilibrium

The Gibbs construction

Neutron star matter is a multi-component system with two conserved ”charges” (electric charge and baryon number)

Global charge neutrality: each of the two phases can have a net and opposite electric charge

→ The two phases can coexist (mixed phase) in a finite range of pressure

The Maxwell construction

One-component system (e.g. water)

Local charge neutrality: each phase in equilibrium is separately charge neutral.

→ Constant pressure in the mixed phase. Since P(r) must be monotonic in NS, there is a sharp density discontinuity in the stellar core at the phase boundary.

N. Glendenning, Phys. Rev. D 46 (1992) 1274

N. Glendenning, Compact Stars, Springer, 1997